Part II

The Search for Engine-Driven Supernovae

CHAPTER 7

The Radio Evolution of the Ordinary Type Ic SN 2002ap[†]

E. Berger[a], S. R. Kulkarni[a], & R. A. Chevalier[b]

[a]Department of Astronomy, 105-24 California Institute of Technology, Pasadena, CA 91125, USA

[b]Department of Astronomy, University of Virginia, P.O. Box 3818, Charlottesville, VA 22903-0818

Abstract

We report the discovery and monitoring of radio emission from the Type Ic SN 2002ap ranging in frequency from 1.43 to 22.5 GHz, and in time from 4 to 50 days after the SN explosion. As in most other radio SNe, the radio spectrum of SN 2002ap shows evidence for absorption at low frequencies, usually attributed to synchrotron self-absorption or free-free absorption. While it is difficult to discriminate between these two processes based on a goodness-of-fit, the *unabsorbed* emission in the free-free model requires an unreasonably large ejecta energy. Therefore, on physical grounds we favor the synchrotron self-absorption (SSA) model. In the SSA framework, at about day 2, the shock speed is $\approx 0.3c$, the energy in relativistic electrons and magnetic fields is $\approx 1.5 \times 10^{45}$ erg and the inferred progenitor mass loss rate is $\approx 5 \times 10^{-7}$ $M_\odot$ yr^{-1} (assuming a 10^3 km sec^{-1} wind). These properties are consistent with a model in which the outer, high velocity supernova ejecta interact with the progenitor wind. The amount of relativistic ejecta in this model is small, so that the presence of broad lines in the spectrum of a Type Ib/c supernova, as observed in SN 2002ap, is not a reliable indicator of relativistic ejecta and hence γ-ray emission.

SECTION 7.1

Introduction

Type Ib/c supernovae (SNe) enjoyed a broadening in interest over the last few years since their compact progenitors (Helium or Carbon stars) are ideal for detecting the signatures of a central engine. Such an engine is expected in the collapsar model (Woosley 1993; MacFadyen et al. 2001), the currently popular model for long-duration γ-ray bursts (GRBs). In this model, the engine (a rotating and accreting black hole) provides the dominant source of explosive power. The absence of an extensive Hydrogen envelope in the progenitor star may allow the jets from the central engine to propagate to the surface and subsequently power bursts of γ-rays.

[†] A version of this chapter was published in *The Astrophysical Journal*, vol. 577, L5–L8, (2002).

Separately, the Type Ic SN 1998bw (Galama et al. 1998a) found in the localization region of GRB 980425 (Pian et al. 2000) ignited interest in "hypernovae"[1] . SN 1998bw is peculiar for three reasons: (i) broad photospheric absorption lines (Iwamoto et al. 1998; Woosley et al. 1999), (ii) a large kinetic energy release, $E_{k,51} \sim 30$ ($E_k = 10^{51} E_{k,51}$ erg is the SN energy), inferred from the optical data and (iii) bright radio emission at early time. Robust equipartition arguments led to an inferred energy of $E_\Gamma \gtrsim 10^{49}$ erg in ejecta with relativistic velocities, $\Gamma \sim$ few (Kulkarni et al. 1998). No other SN has shown hints of such an abundance of relativistic ejecta. Tan et al. (2001) explain the relativistic ejecta as resulting from an energetic shock as it speeds up the steep density gradient of the progenitor. The γ-ray and radio emission would then arise in the forward shock.

From the perspective of a GRB–SN connection, what matters most is the presence of relativistic ejecta. γ-ray emission traces ultra-relativistic ejecta, but as was dramatically demonstrated by SN 1998bw, the radio serves as an equally good proxy, with the added advantage that the emission is not beamed. Given this, we began a systematic program of investigating at radio wavelengths all Ib/c SNe with features similar to SN 1998bw: a hypernova or broad optical lines.

Y. Hirose discovered SN 2002ap in M74 (distance, $d \sim 7.3$ Mpc; Smartt et al. 2002) on 2002, Jan. 29.40 UT (see Nakano et al. 2002). Mazzali et al. (2002) inferred an explosion date of 2002, Jan. 28 ± 0.5 UT. Attracted by the broad spectral features (e.g., Kinugasa et al. 2002; Meikle et al. 2002) we began observing the SN at the Very Large Array (VLA[2]).

SECTION 7.2

Observations

We observed SN 2002ap starting on 2002, February 1.03 UT, and detected a radio source coincident with the optical position at α(J2000)= $01^{\rm h}36^{\rm m}23.92^{\rm s}$, δ(J2000)=$+15^\circ 45' 12.87''$, with a 1-σ uncertainty of 0.1 arcsec in each coordinate (Berger et al. 2002c). A log of the observations and the resulting light curves can be found in Table 7.1 and Figure 7.1, respectively.

7.2.1 The Radio Spectrum of SN 2002ap

The peak radio luminosity of SN 2002ap, $L_p(5\,{\rm GHz}) \sim 3 \times 10^{25}$ erg sec^{-1} Hz^{-1}, is a factor of 20 lower than the typical Ib/c SNe (Weiler et al. 1998), and $\sim 3 \times 10^3$ times lower than SN 1998bw (Kulkarni et al. 1998). The time at which the radio emission peaks at 5 GHz is $t_p \sim 3$ day, which may be compared with 10 days for SN 1998bw , and 10–30 days for the typical Ib/c SNe (Weiler et al. 1998; Chevalier 1998).

The spectral index between 1.43 and 4.86 GHz, $\beta_{1.43}^{4.86}$, ($F_\nu \propto \nu^\beta$) changes from ~ 0.5 before day 6, to ~ -0.3 at $t \approx 15$ days, while $\beta_{4.86}^{8.46}$ holds steady at a value of ≈ -0.9. This indicates that the spectral peak, ν_p, is initially located between 1.43 and 4.86 GHz, and decreases with time. This peak could be due to synchrotron self-absorption (SSA) or (predominantly) free-free absorption (FFA) arising in the circumstellar medium (CSM). Regardless of the dominant source of opacity, the emission for frequencies $\nu > \nu_p$ is from optically-thin synchrotron emission.

Massive stars lose matter via strong stellar winds throughout their life and as a result their CSM is inhomogeneous with density, $\rho(r) \propto \dot{M}_w v_w^{-1} r^{-2}$. Here, r is the distance from the star, $\dot{M}$ is the rate of mass loss, and v_w is the wind speed, which is comparable to the escape velocity from the star. The progenitors of Type II SNe are giant stars which have low $v_w \sim 10$ km s^{-1}. Consequently the CSM is dense and this explains why the FFA model has provided good fits to Type II SNe (e.g., Weiler et al. 1998).

[1] There is no accepted definition for a hypernova. Here we use the term to mean a supernova with an explosion energy significantly larger than 10^{51} erg.

[2] The VLA is operated by the National Radio Astronomy Observatory, a facility of the National Science Foundation operated under cooperative agreement by Associated Universities, Inc.

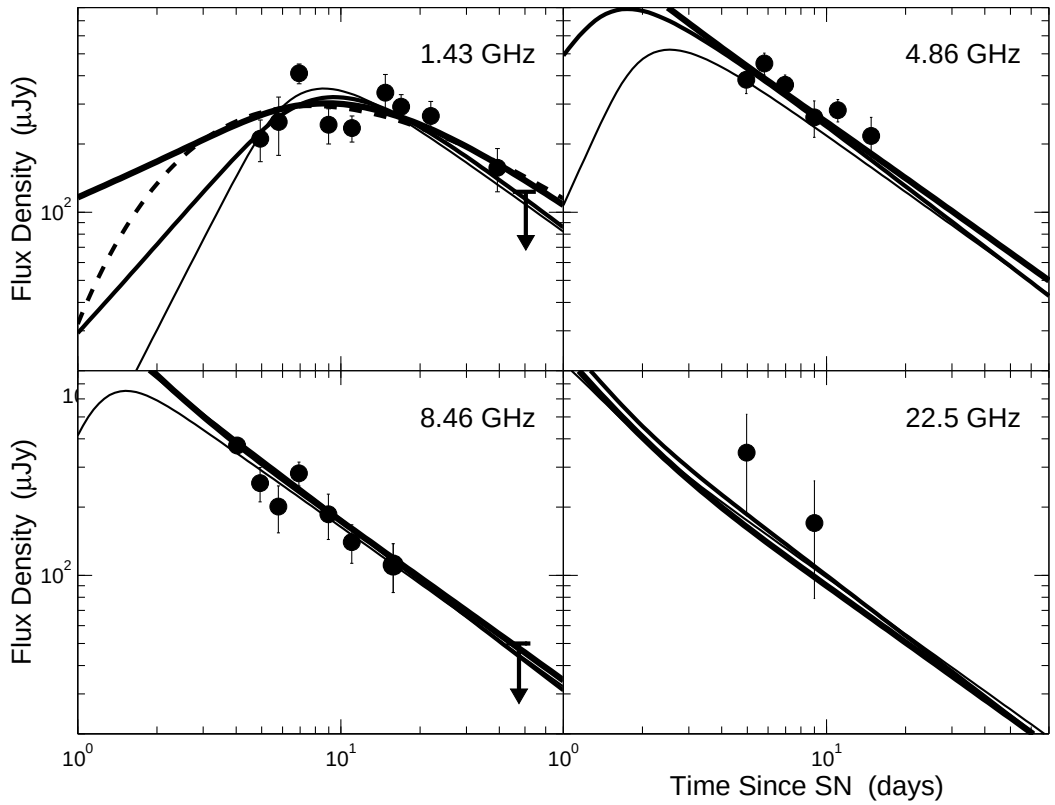

Figure 7.1: Radio light curves of SN 2002ap. The thick solid lines are our three synchrotron self-absorption models described in §7.3, with $\tau_\nu \propto t^{-1.3}$, $\tau_\nu \propto t^{-2.1}$, and $\tau_\nu \propto t^{-3}$ in order of decreasing thickness. The dashed line is the model-fit based on free-free absorption (§7.4). At 4.86, 8.46, and 22.5 GHz, the SSA and FFA models provide the same fit, since the opacity processes do not influence the optically-thin flux. The models diverge in the optically-thick regime, which underlines the importance of rapid, multi-frequency observations.

On the other hand, the progenitors of Type Ib and Ic SNe are compact Helium and Carbon stars which have high escape velocities and therefore fast winds, $\sim 10^3$ km sec^{-1}. Thus, *a priori*, the CSM density is not expected to be high. C98 reviews the modeling of radio emission from Ib/c SNe and concludes that there is little need to invoke free-free absorption. However, synchrotron self absorption is an inescapable source of opacity and must be included in the modeling of Type Ib/c SNe (Chevalier 1998; Kulkarni et al. 1998).

Low-frequency observations provide the simplest way to discriminate between the two models. In the SSA model, the peak frequency is identified with the synchrotron-self absorption frequency, ν_a, and $F_\nu(\nu \lesssim \nu_a) \propto \nu^{5/2}$. In the FFA model, the free-free optical depth is unity at the peak frequency, ν_{ff} and $F_\nu(\nu \lesssim \nu_{ff})$ decreases exponentially. Lacking the requisite discriminatory low frequency data we consider both models.

7.2.2 Robust Constraints

Before performing a detailed analysis, we derive some general constraints using the well-established equipartition arguments (Readhead 1994; Kulkarni et al. 1998). The energy of a synchrotron source with flux density, $F_p(\nu_p)$, can be expressed in terms of the equipartition energy density,

$$\frac{U}{U_{\rm eq}} = \frac{1}{2}\epsilon_B \eta^{11}(1 + \frac{\epsilon_e}{\epsilon_B}\eta^{-17}), \tag{7.1}$$

where $\eta = \theta_s/\theta_{\rm eq}$, the equipartition size is $\theta_{\rm eq} \approx 120 d_{\rm Mpc}^{-1/17} F_{\rm p,mJy}^{8/17} \nu_{\rm p,GHz}^{(-2\beta-35)/34}$ μas, $U_{eq} = 1.1 \times 10^{56} d_{\rm Mpc}^2 F_{\rm p,mJy}^4 \nu_{\rm p,GHz}^{-7} \theta_{\rm eq,\mu as}^{-6}$ erg, and ϵ_e and ϵ_B are the fractions of energy in the electrons and magnetic fields, respectively. In equipartition $\epsilon_e = \epsilon_B = 1$, and it is clear that a deviation from equipartition would increase the energy significantly.

At about day 7, $F_p(\nu_p = 1.4\,{\rm GHz}) \approx 0.3$ mJy (see Figure 7.1). Thus, $\theta_{\rm eq}(t = 7\,{\rm d}) \approx 40$ μas, or $r \approx 4.5 \times 10^{15}$ cm. The resulting equipartition energy is $E_{\rm eq} \approx 10^{45}$ erg, the magnetic field is $B_{\rm eq} \approx 0.2$ G, and the average velocity of the ejecta is $v_{\rm eq} \approx 0.3c$. We note that any other source of opacity (e.g., free-free absorption) would serve to increase $\theta_{\rm eq}$, $E_{\rm eq}$, and $v_{\rm eq}$.

SECTION 7.3

A Synchrotron Self-Absorption Model

The synchrotron spectrum from a source with a power-law electron distribution, $N(\gamma) \propto \gamma^{-p}$ for $\gamma > \gamma_{\rm min}$ is

$$F_\nu = F_{\nu,0}(\nu/\nu_0)^{5/2}(1 - e^{-\tau_\nu})\frac{F_3(\nu,\nu_m,p)}{F_3(\nu_0,\nu_m,p)}\frac{F_2(\nu_0,\nu_m,p)}{F_2(\nu,\nu_m,p)}, \quad (7.2)$$

where the optical depth at frequency ν is given by

$$\tau_\nu = \tau_0(\nu/\nu_0)^{-(2+p/2)}\frac{F_2(\nu,\nu_m,p)}{F_2(\nu_0,\nu_m,p)}, \quad (7.3)$$

and

$$F_\ell(\nu,\nu_m,p) = \int_0^{x_m} F(x)x^{(p-\ell)/2}dx; \quad (7.4)$$

see Li & Chevalier (1999). Here $x_m \equiv \nu/\nu_m$ (Rybicki & Lightman 1979), and ν_m is the characteristic synchrotron frequency of electrons with $\gamma = \gamma_{\rm min}$. The subscript zero indicates quantities at a reference frequency which we set to 1 GHz. Finally, ν_a is defined by the equation $\tau_{\nu_a} = 1$.

The evolution of the synchrotron emission depends on a number of parameters. Following Chevalier (1998), we assume that p, ϵ_e, ϵ_B in the post-shock region remain constant with time; here, $\epsilon_e = \epsilon_B = 0.1$. The evolution of the synchrotron spectrum is sensitive to the expansion radius of the forward shock front, $r_s \propto t^m$, which is related to the density structure of the shocked ejecta and that of the CSM. We allow for these hydrodynamic uncertainties by letting $F_{\nu,0} \propto t_d^{\alpha_F}$ and $\tau_0 \propto t_d^{\alpha_\tau}$, where t_d is the time in days since the SN explosion. In the model adopted here, both these indices depend on m and p. It can be shown that the temporal index of the optically thin flux, $\alpha = \alpha_F + \alpha_\tau$. The synchrotron characteristic frequency, ν_m, is particularly useful for inferring the CSM density, and we parametrize it as $\nu_m = \nu_{m,0} t_d^{\alpha_{\nu_m}}$ GHz where $\nu_{m,0} = \nu_m$ GHz. For typical values of m, and $\rho(r) \propto r^{-2}$, $\alpha_{\nu_m} \approx -0.9$.

With these scalings and Eqs. 7.2–7.4 we carry out a least-squares fit to the data. Given the lack of early optically-thick data (i.e., 1.43 GHz) it is not surprising that our least-squares analysis allows a broad range of values for α_τ. In Figure 7.1 we plot fits spanning the minimum χ^2: $\alpha_\tau = -1.3, -2.1, -3$ (corresponding to $\chi^2 = 40, 43, 46$, respectively and 21 degrees of freedom). We note that for other Ib/c SNe α_τ range from -2 to -3 (Chevalier 1998; Li & Chevalier 1999)

The fits, in conjunction with Eqs. 13–15 of Li & Chevalier (1999) allow us to trace the evolution of r_s, the total (magnetic+electrons) energy (E), and the electron density (n_e) in the shock (Figure 7.2). We find that for $\alpha_\tau = -1.3$, $r_s \propto t^{0.25}$ i.e., the blastwave decelerates. However, $\alpha_\tau = -3$ provides the expected $r_s \propto t^{0.9}$. Adopting this physically reasonable model, we obtain: $\tau_0(t) = 1.2 \times 10^3 t_d^{-3}$, $F_{\nu,0}(t) = 2.9 t_d^{2.2}$ μJy, and $p = 2$. From Figure 7.2 we note that the early shock velocity is high, $0.3c$, regardless of the choice of α_τ, and close to that derived from the simple equipartition arguments (§7.2.2).

The mass loss rate of the progenitor star is estimated from r_s and n_e, $\dot{M}_w = 8\pi\zeta n_e m_p r^2 v_w \approx 9 \times 10^{-9} \nu_{m,0}^{-0.8}$ M$_\odot$ yr^{-1}, where the compression factor is $\zeta = 1/4$, the nucleon-to-electron ratio is taken to be 2 and $v_w = 10^3$ km sec^{-1}. Knowing B_{eq} and our assumed ϵ_e we find $\nu_m \sim 10^7$ Hz and thus

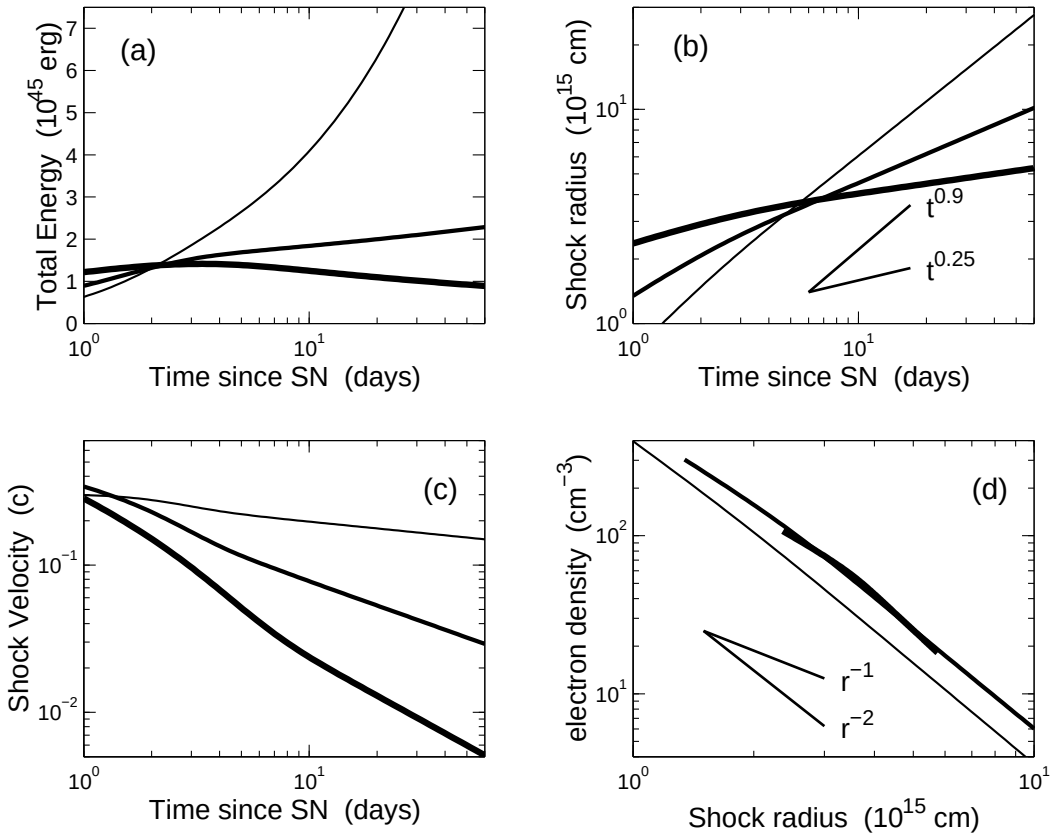

Figure 7.2: Inferred physical parameters based on the synchrotron self-absorption models described in §7.3. The panels are (a) time evolution of the total energy, (b) radius of the radio photosphere, (c) electron density in the shock as a function of radius, and (d) velocity of the shock front as a function of time. Models with $\tau_\nu \propto t^{-1.3}$, $\tau_\nu \propto t^{-2.1}$, and $\tau_\nu \propto t^{-3}$ are shown in order of decreasing thickness. The most likely fit is the one following $r \propto t^{0.9}$ (i.e., the model with $\tau_\nu \propto t^{-3}$).

$\dot{M}_w \approx 5 \times 10^{-7}\, M_\odot$ yr^{-1} – similar to that inferred for SN 1998bw Li & Chevalier (1999).

There are two consistency checks. First, with this $\dot{M}_w$, free-free absorption is negligible. Second, the kinetic energy of the swept-up material is 2×10^{46} erg – consistent with our estimate of the equipartition energy and ϵ_e.

7.3.1 The SSA Model in the Context of a Hydrodynamic Model

The results of §7.3 can be tied in to a fairly simple hydrodynamic model. Matzner & McKee (1999) show that for the progenitors of Ib/c SNe (compact stars with radiative envelopes) the ejecta post-explosion density profile can be described by power laws at low and high velocities, separated by a break velocity, $v_{\rm ej,b} = 5150(E_{k,51}/M_1)^{1/2} \approx 2 \times 10^4$ km sec^{-1}; here the mass of the ejecta is $M_{\rm ej} = 10 M_1\, M_\odot$. We use $E_{k,51} \approx 4 - 10$ and $M_1 \approx 0.25 - 0.5$ for SN 2002ap (Mazzali et al. 2002). At $v_s \approx 0.3c$, the density profile is given by $\rho_s \approx 3 \times 10^{96} E_{k,51}^{3.59} M_1^{-2.59} t^{-3} v^{-10.18}$ g cm^{-3}. This profile extends until radiative losses become important when the shock front breaks out of the star. Using Eq. 32 of Matzner & McKee (1999) this happens for $v_s \approx 1.5c$ (assuming a typical 1 R$_\odot$ radius for the progenitor star). Thus, the outflow can become relativistic.

Using the self-similar solution of Chevalier (1982) the velocity of the outer shock radius, R, (assuming a $\rho = Ar^{-2}$ CSM) is

$$\frac{R}{t} = 52,300\, E_{k,51}^{0.44} M_1^{-0.32} A_*^{-0.12} t_d^{-0.12} \text{ km sec}^{-1}, \tag{7.5}$$

where $A_* = (\dot{M}_w/10^{-5}\ M_\odot\ \mathrm{yr}^{-1})(v_w/10^3\ \mathrm{km\ sec}^{-1})^{-1}$. The shock velocity, $\dot{R}$, is insensitive to the circumstellar wind density. Thus, we find that the velocities inferred from the radio observations of SN 2002ap can be naturally accounted for by the outer supernova ejecta.

The energy above some velocity V is

$$E(v > V) \approx \int_V^\infty \frac{1}{2}\rho_f v^2 4\pi v^2 t^3 dv = 7.2 \times 10^{44} E_{k,51}^{3.59} M_1^{-2.59} V_5^{-5.18}\ \mathrm{ergs}, \tag{7.6}$$

where v_5 is the velocity in units of 10^5 km s^{-1}. For the preferred SN 2002ap parameters, $E(v > V) \approx 3.8 \times 10^{48} V_5^{-5.18}$ erg. There is therefore plenty of energy in the high velocity ejecta to account for the observed radio emission, and in fact a kinetic energy, $E_{k,51} = 0.5$, would be sufficient.

Given the over-abundance of $E(v > V_5)$ relative to the energy inferred from the radio emission, we wonder how secure are the estimates of $E_{k,51}$ and M_1 of Mazzali et al. (2002). In particular, these parameters are derived from early optical observations and are subject to asymmetries in the explosion. For SN 1998bw, the asymmetric model of Höflich et al. (1999) yielded $E_{k,51} \sim 2$, an order of magnitude smaller than that obtained from symmetrical models (e.g., Iwamoto et al. 1998).

7.3.2 Interstellar Scattering & Scintillation

Interstellar scattering and scintillation (ISS) is expected for radio SNe (cf. Kulkarni et al. 1998). Indeed, the perceptible random deviations from the model curves (see Figure 7.1), which account for the high $\chi^2_{\rm min}$ could arise from ISS.

Using the ISS model of Goodman (1997), and the Galactic free electron model of Taylor & Cordes (1993), we estimate $m_{8.46} \approx 5\%$, $m_{4.86} \approx 10\%$, and $m_{1.43} \approx 40\%$; m_ν is the modulation index (the ratio of the rms to the mean) for each frequency.

We estimate the actual modulation index empirically by adding $m_\nu F_\nu$ in quadrature to each measurement error so that the reduced $\chi^2_{\rm min}$ is unity. Here F_ν is the model flux described in §7.3. We find $m_{8.46} \approx 10\%$, $m_{4.86} \approx 20\%$, and $m_{1.43} \approx 30\%$, in good agreement with the theoretical estimates. This provides an independent confirmation of the size, and hence expansion velocity of the ejecta. We note that since the modulation is not severe in any of the bands, the results of §7.3 are quite robust.

SECTION 7.4

A Free-Free Absorption Model

In this model, the spectrum is parametrized as (Chevalier 1984; Weiler et al. 1986):

$$\begin{aligned} F_\nu &= K_1 \nu_5^\beta t_d^\alpha\, e^{-\tau_\nu} \\ \tau_\nu &= K_2 \nu_5^{-2.1} t_d^\delta, \end{aligned} \tag{7.7}$$

where $\nu_5 = 5\nu$ GHz. We find an acceptable fit ($\chi^2 = 40$ for 21 degrees of freedom) yielding: $K_1 \approx 2$ mJy, $K_2 \approx 0.4$, $\alpha \approx -0.9$, $\beta \approx -0.9$, and $\delta \approx -0.8$. With these parameters and Eq. 16 of Weiler et al. (1986) we find $\dot{M}_w \approx 5 \times 10^{-5}$ M$_\odot$ yr^{-1} for $v_w = 10^3$ km sec^{-1}.

Using our derived parameters, one day after the explosion $\nu_{\rm ff} \approx 3.2$ GHz, and $F_\nu(\nu_{\rm ff}) \approx 1.1$ mJy (Figure 7.1). The unabsorbed flux at the peak of the synchrotron spectrum is $F_\nu(\nu_a) \approx 3(\nu_a/3.2\,\mathrm{GHz})^{-0.9}$ mJy (note $\nu_a < \nu_{ff}$ in the FFA model) for which $r_{\rm eq} \approx 7.5 \times 10^{15}(\nu_a/3.2\,\mathrm{GHz})^{-3/2}$ cm. Thus $v_{\rm eq} \approx 3c(\nu_a/3.2\,\mathrm{GHz})^{-3/2}$, which corresponds to $\Gamma = 2(\nu_a/3.2\,\mathrm{GHz})^{-1}$ if relativistic effects are taken into account (R. Sari priv. comm.). Alternatively, if we fix the expansion velocity to the optical value, $v_s \approx 3 \times 10^4$ km sec^{-1} (Mazzali et al. 2002), we find a brightness temperature, $T_b \approx 4 \times 10^{13}$ K — clearly in excess of the equipartition temperature, again necessitating a high bulk Lorentz factor, $\Gamma \sim 10^2$.

Thus, even if $\nu_a = \nu_{\rm ff}$ (in which case free-free opacity would not be necessary in the first place), the FFA model requires truly relativistic ejecta, or alternatively a large departure from equipartition,

resulting in $E \approx 7 \times 10^{50} (\nu_a / 3.2\,\mathrm{GHz})^{-9}$ erg (for $v_s \approx 0.5c$ instead of $3c$). Clearly, the energy requirement would increase by many orders of magnitude if $\nu_a \ll \nu_{\rm ff}$.

SECTION 7.5

Discussion and Conclusions

SN 1998bw exhibited broad photospheric absorption lines and bright radio emission. These two peculiarities made sense in that the simple theory suggested that broad photospheric features are a reliable indicator of relativistic ejecta, a necessary condition for γ-ray emission.

The type Ic SN 2002ap elicited much interest because it too displayed similar broad lines. However, from our radio observations we estimate the energy in relativistic electrons and magnetic fields to be quite modest: $E \approx 2 \times 10^{45}$ ergs in ejecta with a velocity $\approx 0.3c$. Both the energy and speed of the ejecta can be accounted for in the standard hydrodynamical model. Thus, our principal conclusion is that broad photospheric lines are not good predictors of relativistic ejecta.

Moreover, the broad photospheric features led modelers to conclude that SN 2002ap was a hypernova with an explosion energy of $E_{51} \sim 4 - 10$ erg (Mazzali et al. 2002). However, the radio observations suggest that SN 2002ap is not an energetic event. In the same vein, we note that Kawabata et al. (2002) suggest, based on spectro-polarimetric observations, a jet with a speed of $0.23c$ and carrying 2×10^{51} erg. Such a jet, regardless of geometry, would have produced copious radio emission.

We end with two conclusions. First, at least from the perspective of relativisic ejecta, SN 2002ap was an ordinary Ib/c SN. Second, broad photospheric lines appear not to be a good proxy for either an hypernova origin or γ-ray emission.

Dale Frail was involved in various aspects of this project and we are grateful for his help and encouragement. We also wish to acknowledge useful discussions with J. Craig Wheeler. Finally, we thank NSF and NASA for supporting our research.

Table 7.1. Radio Observations of SN 2002ap

Epoch (UT)	$F_{1.43} \pm \sigma$ (μJy)	$F_{4.86} \pm \sigma$ (μJy)	$F_{8.46} \pm \sigma$ (μJy)	$F_{22.5} \pm \sigma$ (μJy)
2002 Feb 1.03	—	—	374 ± 29	—
2002 Feb 1.93	211 ± 44	384 ± 50	255 ± 44	348 ± 165
2002 Feb 2.79	250 ± 72	453 ± 50	201 ± 47	—
2002 Feb 3.93	410 ± 41	365 ± 38	282 ± 34	—
2002 Feb 5.96	243 ± 43	262 ± 48	186 ± 42	170 ± 91
2002 Feb 8.00	235 ± 31	282 ± 32	140 ± 27	—
2002 Feb 11.76	337 ± 68	217 ± 45	111 ± 27	—
2002 Feb 13.94	292 ± 38	—	—	—
2002 Feb 18.95	266 ± 42	—	—	—
2002 Mar 4.85+11.83	157 ± 34	—	—	—
2002 Mar 18.77+19.97	57 ± 33	—	25 ± 25	—

Note. — The columns are (left to right), (1) UT date of each observation, and flux density and rms noise at (2) 1.43 GHz, (3) 4.86 GHz, (4) 8.46 GHz, and (5) 22.5 GHz. Observations with more than one date have been co-added to increase the signal-to-noise of the detection.

CHAPTER 8

A Radio Survey of Type Ib and Ic Supernovae: Searching for Engine Driven Supernovae†

E. Berger[a], S. R. Kulkarni[a], D. A. Frail[b] & A. M. Soderberg[a]

[a]Department of Astronomy, 105-24 California Institute of Technology, Pasadena, CA 91125, USA

[b]National Radio Astronomy Observatory, P. O. Box 0, Socorro, NM 87801

Abstract

The association of γ-ray bursts (GRBs) and core-collapse supernovae (SNe) of Type Ib and Ic was motivated by the detection of SN 1998bw in the error box of GRB 980425 and the now-secure identification of SN 2003dh in the cosmological GRB 030329. The bright radio emission from SN 1998bw indicated that it possessed some of the unique attributes expected of GRBs, namely, a large reservoir of energy in (mildly) relativistic ejecta and variable energy input. The two popular scenarios for the origin of SN 1998bw are a typical cosmological burst observed off-axis or a member of a new distinct class of supernova explosions (GRB Supernovae, or gSNe). In the former, about 0.5% of local Type Ib/c SNe are expected to be similar to SN 1998bw; for the latter no such constraint exists. Motivated thus, we began a systematic program of radio observations of most reported Type Ib/c SNe accessible to the Very Large Array. Of the 33 SNe observed from late 1999 to the end of 2002 at most one is as bright as SN 1998bw. From this we conclude that the incidence of such events is $\lesssim 3\%$. Furthermore, analysis of the radio emission indicates that none of the observed SNe exhibit clear engine signatures. Finally, a comparison of the SN radio emission to that of GRB afterglows indicates that none of the SNe could have resulted from a typical GRB, independent of the initial jet orientation. Thus, while the nature of SN 1998bw remains an open question, there appears to be a clear dichotomy between the majority of hydrodynamic and engine-driven explosions.

SECTION 8.1

Introduction

The death of massive stars and the processes that lead to the formation of the compact remnants is a forefront area in stellar astrophysics. Recent advances in modeling suggest that great diversity can be expected. Indeed, observationally we have already witnessed a large diversity in the neutron star remnants: radio pulsars, AXPs, SGRs, and the central source in Cas A. We know relatively little about the formation of black holes, static or rotating.

† A version of this chapter was published in *The Astrophysical Journal*, vol. 599, 408–418, (2003).

The compact objects form following the collapse of the progenitor core. The energy of the resulting explosion can be supplemented, or even dominated, by the energy released from the compact object (e.g., a rapidly rotating magnetar or an accreting black hole). Such "engines" can drive strongly collimated outflows (MacFadyen & Woosley 1999), but even in their absence the core collapse process appears to be mildly asymmetric (e.g., Wang et al. 2001). Regardless of the source of energy, a fraction of the total energy, E_K, is coupled to the debris or ejecta (mass $M_{\rm ej}$) and it is these two gross parameters which determine the appearance and evolution of the resulting explosion. Equivalently one may consider E_K and the mean initial speed of ejecta, v_0, or the Lorentz factor, $\Gamma_0 = [1 - \beta_0^2]^{-1/2}$, where $\beta_0 = v_0/c$.

Supernovae (SNe) and γ-ray bursts (GRBs), are distinguished by their ejecta velocities. In the former $v_0 \sim 10^4$ km s^{-1} as inferred from optical absorption features (e.g., Filippenko 1997), while for the latter $\Gamma_0 \gtrsim 100$, inferred from the non-thermal prompt emission (Goodman 1986; Paczynski 1986), respectively. The large difference in initial velocity arises from significantly different ejecta masses: $M_{\rm ej} \sim few$ M$_\odot$ in SNe compared to $\sim 10^{-5}$ M$_\odot$ in GRBs.

In the conventional interpretation, $M_{\rm ej}$ for SNe is large because E_K is primarily derived from the mildly asymmetrical collapse of the core and the energy thus couples to most the mass left after the formation of the compact object. Mysteriously, E_K clusters around 1 FOE (FOE is 10^{51} erg) in most SNe, a mere 1% of the energy released in the gravitational collapse of the core.

Whereas the initial ejecta speed is solely determined by E_K and $M_{\rm ej}$, a fraction of the ejecta is accelerated to higher velocities as the blast wave races down the density gradient of the stellar enveloped (e.g., Matzner & McKee 1999). For the wind- or binary-stripped (e.g., Uomoto 1986; Branch et al. 1990; Woosley et al. 1993; Nomoto et al. 1994) helium and carbon progenitors of Type Ib and Ic SNe, both factors (a smaller core mass and a steep density gradient) conspire to produce ejecta at velocities as high as $\Gamma\beta \sim 1$. However, only $\lesssim 10^{-5} E_K$ is carried by these ejecta (Colgate 1968; Woosley & Weaver 1986; Matzner & McKee 1999). In contrast, high velocity ejecta is neither expected nor observed in Type II SNe with their massive stellar envelopes.

GRB models, on the other hand, appeal to a stellar mass black hole remnant, which accretes matter on many dynamical timescales and powers relativistic jets (the so-called collapsar model; Woosley 1993; MacFadyen & Woosley 1999); highly magnetized neutron stars have also been proposed (e.g., Ruderman et al. 2000). Observationally, this model is supported by the association of some GRBs with SN explosions (e.g., Stanek et al. 2003). In addition, the complex temporal profiles and long duration of GRBs are interpreted in terms of an engine that is relatively long lived (i.e., not a singular explosion). The high Lorentz factors, a high degree of collimation with opening angles of a few degrees (Frail et al. 2001), and episodes of energy addition presumably from shells of ejecta with varying Lorentz factors, further distinguish GRBs from Type Ib/c SNe.

We now recognize that engine-driven events – GRBs and the recently discovered X-ray Flashes – in fact have a wide dispersion in their ultra-relativistic output as manifested by their beaming-corrected γ-ray energies (Bloom et al. 2003b) and X-ray luminosities (Berger et al. 2003a). However, these cosmological explosions appear to have a nearly constant total explosive yield when taking into account the energy in mildly relativistic ejecta (Berger et al. 2003c).

The unusual and nearby ($d \sim 40$ Mpc) SN 1998bw shares some of the unique attributes expected of GRBs. This Type Ic SN was found to be coincident in time and position with GRB 980425 (Galama et al. 1998a), an event with a single smooth profile. The inferred isotropic energy in γ-rays of GRB 980425 was only 8×10^{47} erg (Pian et al. 2000), three to six orders of magnitude fainter than typical GRBs. More importantly, SN 1998bw exhibited unusually bright radio emission indicating about 10^{50} erg of mildly relativistic ejecta (Li & Chevalier 1999). Equally significant, the radio emission indicated a clear episode of energy addition[1] (Li & Chevalier 1999). None of these features – γ-rays, significant energy with $\Gamma\beta \gtrsim 2$, and episodes of energy addition – have been seen in any other nearby SN. Thus, the

[1] With the assumption that free-free absorption is the dominant absorption process, the increase in flux has also been interpreted as due to variations in the circumstellar density (Weiler et al. 2001). However, the model proposed by these authors requires unrealistic expansion velocities and/or kinetic energies.

empirical data strongly favor an engine origin for SN 1998bw. In the optical, SN 1998bw also appears to be extreme: velocity widths approaching 60,000 km s^{-1} were seen at early time (Iwamoto et al. 1998) and the inferred explosion energy may be above normal values, with estimates ranging from 2 to 50 FOE (Höflich et al. 1999; Nakamura et al. 2001).

The inference of an engine in SN 1998bw raises two scenarios for its origin and relation to GRBs. GRB 980425 may have been a typical burst but viewed well away from the jet axis (hereafter, the off-axis model), thereby resulting in apparently weak γ-ray emission despite the great proximity. Alternatively, SN 1998bw represents a different class of SNe. If so, collapsars can produce very diverse explosions.

A powerful discriminant between these two scenarios is the expected rate of SN 1998bw-like events. In the off-axis model, the fraction of Type Ib/c SNe that are powered by a central engine is linked to the mean beaming factor of GRBs (e.g., Frail et al. 2001; Totani & Panaitescu 2002). Recently, Frail et al. (2001) presented the distribution of jet opening angles for a sample of 15 GRBs, and found that the mean beaming factor is $\langle f_b^{-1} \rangle \sim 500$; here $f_b = [1 - \cos(\theta_j)]$ is the beaming fraction, and θ_j is the collimation angle. With an estimated local GRB rate of ~ 0.5 Gpc^{-3} yr^{-1} (Schmidt 2001) compared to a Type Ib/c SN rate of $\sim 4.8 \times 10^4$ Gpc^{-3} yr^{-1} (Marzke et al. 1998; Cappellaro et al. 1999; Folkes et al. 1999), we expect that $\sim 0.5\%$ of Type Ib/c SNe will be similar[2] to SN 1998bw.

On the other hand, if SN 1998bw is not an off-axis cosmological burst, then the rate of similar events has to be assessed independent of the GRB rate. An upper limit can be obtained by assuming that all Type Ib/c SNe are engine driven highly asymmetric explosions with SN 1998bw having the most favorable geometry. In this context, Norris (2002) has argued that of the 1429 long-duration BATSE bursts, about 90 events possess similar high-energy attributes as that of GRB 980425. This sub-sample may be concentrated along the super-galactic plane. If this sub-sample is accepted as distinct from the cosmological bursts then $\sim 25\%$ of Type Ib/c SNe within 100 Mpc are expected to be events like SN 1998bw.

Here, we report a comprehensive program of radio observations of nearby Type Ib/c SNe. We began this program in 1999 (motivated by SN 1998bw) and observed most reported Type Ib/c SNe with the Very Large Array. Our basic hypothesis is that (mildly) relativistic ejecta are best probed by radio observations, as was demonstrated in the case of SN 1998bw. Furthermore, radio observations of Type Ib/c SNe allow us to directly compare these objects to the radio afterglows of cosmological GRBs. Thus, we can empirically (direct comparison of radio luminosity distributions) and quantitatively (calorimetry via radio observations) investigate the link, or lack thereof between Type Ib/c SNe and cosmological GRBs. As alluded to above, we did not investigate Type II SNe since the extended envelopes and dense circumstellar media of their progenitors are reasonably expected to mask the activity of a putative engine and thus suppress the presence of mildly relativistic ejecta to which we are most sensitive.

The organization of the paper is as follows. In §8.2 we present the details of the observations. The results are summarized in §8.3, where we investigate the broad radio properties (§8.3.1), expansion velocities (§8.3.2), and energies in high velocity ejecta (§8.3.3). We further provide a comparison to the radio afterglows of GRBs in §8.4 and draw conclusions in §8.5.

SECTION 8.2

Observations

Table 8.1 summarizes the Very Large Array (VLA[3]) observations of Type Ib/c SNe starting in late 1999 and up to the end of 2002. We observed a total of 33 SNe out of 51 identified spectroscopically during the same period. The observed targets were determined solely by the availability of observing time and optical selection criteria; we did not employ any additional selection criteria.

[2] We note that this fraction may be somewhat higher in jet models in which the energy and/or Lorentz factor decrease away from the jet axis. The exact fraction depends on the details of the energy and Lorentz factor distribution (Rossi et al. 2002; Zhang & Mészáros 2002).

[3] The VLA is operated by the National Radio Astronomy Observatory, a facility of the National Science Foundation operated under cooperative agreement by Associated Universities, Inc.

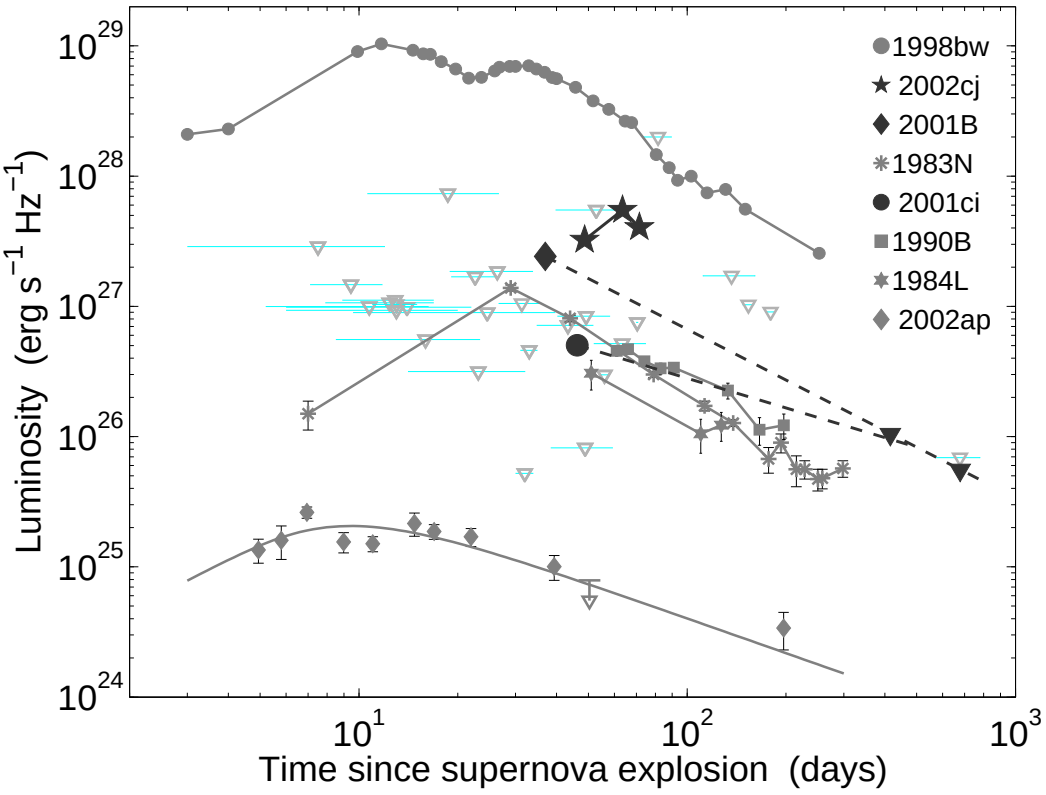

Figure 8.1: Radio light curves of Type Ib/c SNe detected in this survey and from the literature, as well as upper limits for the non-detections (triangles); these are plotted as 3σ in most cases with the exception of SNe which are located on top of a bright host galaxy (see Table 8.1). The light curves are at 8.5 GHz (SN 1998bw), 4.9 GHz (SNe 1983N, 1984L, and 1990B), and 1.4 GHz (SN 2002ap); these frequencies were chosen since they provide the best coverage of the radio evolution. For SN 2002ap we plot the model of Berger et al. (2002b), while the other solid lines simply trace the observations and do not represent a model fit. The uncertainty in time for the non-detections represents the uncertain time of explosion. We note that for SN 2002cg, which is the only SN that is potentially brighter than SN 1998bw, the limit is 10σ due to the superposition of the SN on top of its host galaxy.

In all observations we used the standard continuum mode with 2×50 MHz bands, centered on 1.43, 4.86, or 8.46 GHz. We used the sources 3C 48 (J0137+331), 3C 147 (J0542+498), and 3C 286 (J1331+305) for flux calibration, and calibrator sources within $\sim 5^\circ$ of the SNe to monitor the phase. The data were reduced and analyzed using the Astronomical Image Processing System (Fomalont 1981).

SECTION 8.3

Population Statistics

In this section we investigate the ejecta properties and diversity of the sample. Results for individual SNe are given in the Appendix. In Figure 8.1 we plot the radio luminosities and upper limits for Type Ib/c SNe observed in this survey and in the past (SN 1983N: Sramek et al. 1984; SN 1984L: Panagia et al. 1986; Weiler et al. 1986; SN 1990B: van Dyk et al. 1993; SN 1998bw: Kulkarni et al. 1998; SN 2002ap: Berger et al. 2002b). The typical delay between the SN explosion and time of our observations is about 20 days, with four SNe observed with a delay of over 100 days. In addition, three of the SNe are embedded in host galaxies with strong radio emission. For these cases, we adopt upper limits that correspond to the brightness of the galaxy (at least ten times the root-mean-square noise of the individual image). Four of the thirty three SNe have been detected. Thus the detection rate of our

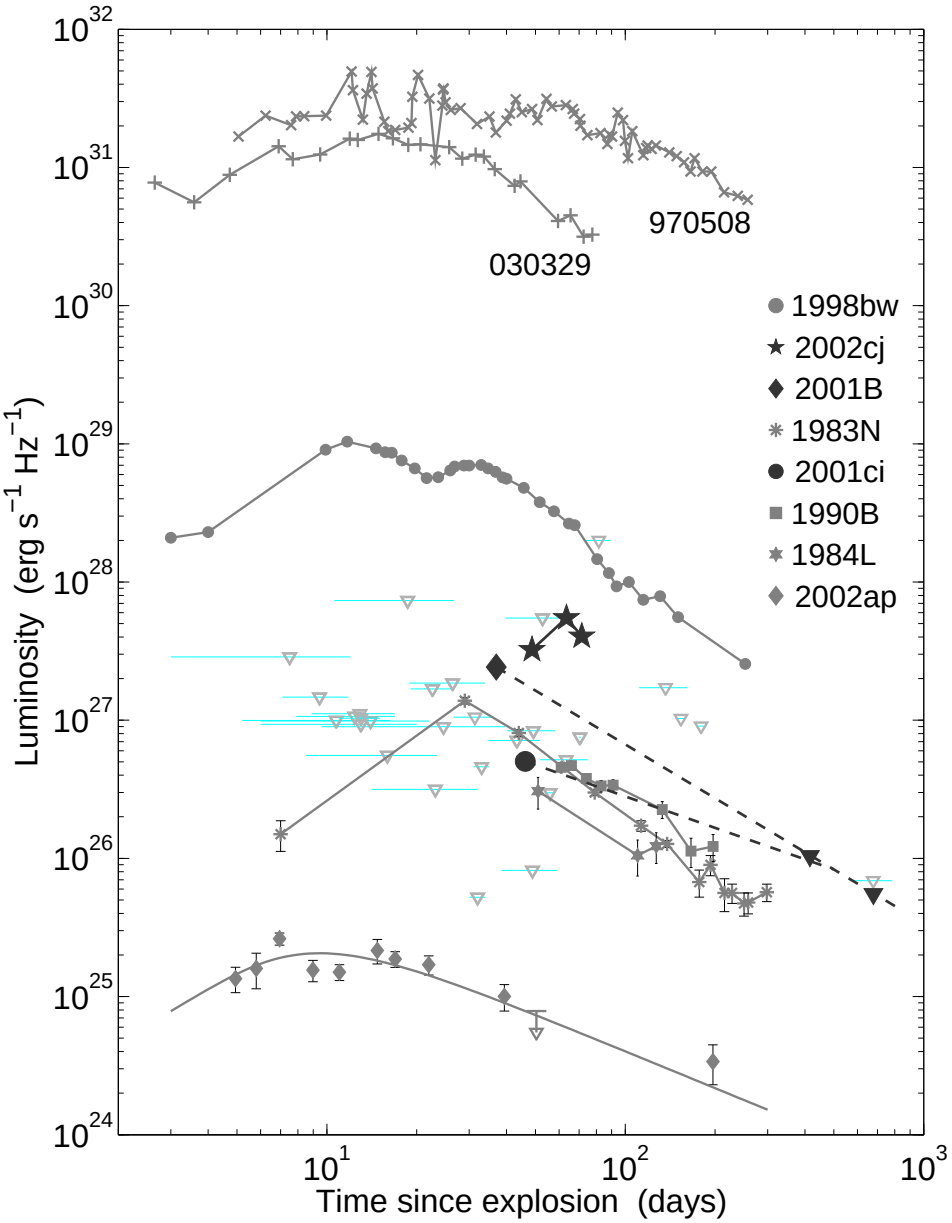

Figure 8.2: Same as Figure 8.1 but including the 8.46 GHz light curves of GRB 970508 (Frail et al. 2000c) and GRB 030329 (Berger et al. 2003c). These GRB afterglows are at least two orders of magnitude brighter than SN 1998bw, the brightest Type Ib/c SN. We note that the fluctuations in the GRB light curves are not intrinsic, and arise instead from interstellar scintillation. Based on the significant difference in radio luminosity we rule out the possibility that the Type Ib/c SN observed here produced a GRB. This is discussed more quantitatively in in §8.4 and Figures 8.4 and 8.5.

experiment with a typical flux density limit of 0.15 mJy (3σ) is about 12%.

8.3.1 Radio Properties of Type Ib/c SNe

Figure 8.1 provides a succinct summary of the radio light curves of the Type Ib/c SNe. Two strong conclusions can be immediately drawn from this Figure. First, SNe as bright as SN 1998bw are rare. Second, there is significant dispersion in the luminosities of Type Ib/c SNe, ranging from $L_{\nu,\rm rad} \approx 10^{29}$ erg s^{-1} Hz^{-1} at the bright end (SN 1998bw) to that of SN 2002ap which is fainter by about four orders

of magnitude (Berger et al. 2002b). It is curious that SN 2002ap also happens to be the nearest Ib/c SN in our sample (Table 8.1). Six of the eight Type Ib/c SNe detected in the radio to date cluster in the range of about $(3-50)\times10^{26}$ erg s^{-1} Hz^{-1}. This may be partly due to a selection effect since the typical detection threshold is about $4\times10^{26}(d/50\,\mathrm{Mpc})^2$ erg s^{-1} Hz^{-1}.

We also find that 28 of the 29 non-detections are no brighter than 0.1 times the luminosity of SN 1998bw. SN 2002cg appears potentially brighter than SN 1998bw only because it is embedded in a radio bright host galaxy; we are therefore forced to use a 10σ limit on its luminosity (Table 8.1). Thus, the incidence of bright events like SN 1998bw is $\lesssim 3\%$.

As with the radio luminosities, the peak times also exhibit great variation: at 1.4 GHz the emission from SN 2002ap peaked at about 7 days, while for SN 2002cj it peaked at about 65 days. For SN 1998bw the initial peak occurred at 15 days, followed by a second peak at about 40 days. Similarly, at 8.5 GHz, SN 1998bw peaked at 12 and 30 days past explosion, SN 1983N peaked at about 30 days, and SN 2002ap is predicted to have peaked at $\sim 1-2$ days (the first observation at this frequency was taken about 4 days after the SN explosion).

8.3.2 Expansion Velocities

If the radio emission arises from a synchrotron spectrum peaking at the self-absorption frequency, ν_a, then the peak time and peak luminosity directly measure the mean expansion speed (Chevalier 1998). This is simply because the self-absorption frequency is sensitive to the size of the source, while the luminosity is sensitive to the swept-up mass. We use Equation 16 of Chevalier (1998) to evaluate the average expansion velocities:

$$v_p \approx 3.1\times10^4 L_{p,26}^{17/36} t_{p,10}^{-1} \nu_{p,5}^{-1}\ \mathrm{km\,s^{-1}}. \quad (8.1)$$

Here, $L_p = 10^{26}L_{p,26}$ erg s^{-1} Hz^{-1} is the peak luminosity, $t_p = 10t_{p,10}$ days is the time of peak emission relative to the SN explosion, and $\nu_p = 5\nu_{p,5}$ GHz is the peak frequency. We infer velocities ranging from $v\sim10^4$ to 10^5 km s^{-1} (Figure 8.3). Again, as with the luminosities, SN 1998bw with $v\sim c$ is an exception.

We note that if free-free absorption plays a significant role, then ν_p is only an upper limit to ν_a, and L_p is a lower limit to the intrinsic peak luminosity. In this case, the inferred values of v_p listed above will in fact be a lower limit to the actual expansion velocity. However, this is probably not significant for Type Ib/c SNe since their compact progenitors have high escape velocities and therefore fast winds and low circumburst densities. Indeed, there is no evidence for free-free absorption either for SN 1998bw (Kulkarni et al. 1998; Li & Chevalier 1999) or SN 2002ap (Berger et al. 2002b).

Estimating the expansion velocities for the non-detections is not straightforward since we cannot ensure that the limits constrain the peak luminosity. We are therefore forced to make an additional assumption. For example, if we assume that most Type Ib/c SNe are similar in their emission properties to SN 1983N, then the majority of upper limits approximately sample the peak emission and the inferred upper limits are $\lesssim 0.3c$ (Figure 8.3).

On the other hand, if the typical peak time is only a few days then our observations only constrain the decaying portion of the light curve and the expansion velocity may be higher. Fortunately, this is not a significant problem based on the following argument. The equipartition energy directly depends on the peak luminosity, $U_{\rm eq}\approx 3.7\times10^{46}L_{p,27}^{20/17}$ erg (see §8.6.3), where $L_p = 10^{27}L_{p,27}$ erg s^{-1} is the peak luminosity at 8.5 GHz. With a typical fading rate of $F_\nu\propto t^{-1}$ in the optically thin regime, there are a few SNe that could have reached a peak luminosity of the order of 10^{29} erg s^{-1} if $t_p = 1$ day post explosion. This is a reasonable minimum peak time taking into account the deceleration time of the ejecta. Thus, the equipartition energy is at most 10^{49} erg, about two orders of magnitude lower than typical GRBs (§8.5). For most non-detections the limit is in fact much lower, $\sim 5\times10^{46}$ to 10^{48} erg. This indicates that a few of the non-detected sources may have in fact produced mildly relativistic ejecta, but these would still be energetically uninteresting when compared to SN 1998bw let alone GRB afterglows.

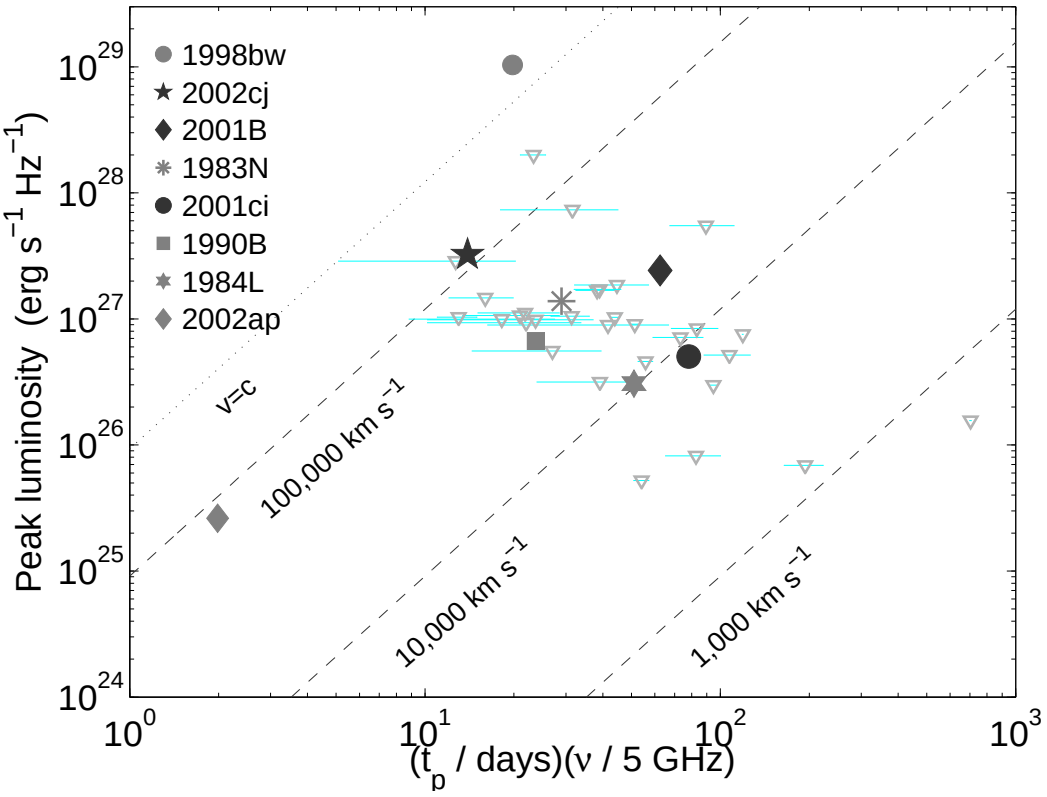

Figure 8.3: Peak radio luminosity plotted versus the time of peak luminosity for Ib/c SNe studied in this survey and from the literature. Symbols are as in Figure 8.1. The diagonal lines are contours of constant average expansion velocity based on the assumption that the peak of the radio luminosity occurs at the synchrotron self-absorption frequency (Chevalier 1998). While the upper limits do not necessarily measure the peak of the spectrum at the time of the observation, a comparison to SN 1983N indicates that the range of time delays relative to the SN explosion reasonably samples the peak. Upper limits measured at $t \gtrsim 100$ days probably miss the peak of the synchrotron spectrum and therefore do not provide a useful limit.

8.3.3 Energetics

In the previous section we found that no SN observed to date is comparable to SN 1998bw especially in regard to the mean expansion speed. SN 1998bw was also interesting because it possessed an unusually large amount of energy in mildly relativistic ejecta. However, a purely hydrodynamic explosion can also produce *some* amount of relativistic ejecta. The energy of such ejecta can be estimated using well understood models of shock propagation in the pre-supernova cores (Chevalier 1982; Matzner & McKee 1999). The key parameters are E_K and $M_{\rm ej}$ which can be inferred from the optical light curves and spectra using hydrodynamic models of a SN explosion in a CO core coupled with radiative transfer calculations (e.g., Iwamoto et al. 2000).

In this section, we investigate whether any of the detected Type Ib/c SNe possess such large energy in high velocity ejecta that cannot be explained by the simplest hypothesis of a purely hydrodynamic explosion. To this end, in Table 8.2 we summarize the results of hydrodynamic models for the SNe that have been detected in the radio.

The ejecta produced in a hydrodynamic explosion has a density profile that can be described by power laws at low and high velocities, separated by a break velocity, which for Type Ib/c progenitors is given by (Matzner & McKee 1999):

$$v_{\rm ej,b} \approx 5.1 \times 10^3 (E_{K,51}/M_{\rm ej,1})^{1/2}\,{\rm km\,s^{-1}}. \quad (8.2)$$

Here $E_K = 10^{51} E_{K,51}$ erg and $M_{\rm ej} = 10 M_{\rm ej,1}$ M$_\odot$. For typical values of E_K and $M_{\rm ej}$, the radio emission from the detected SNe is produced by ejecta above the break velocity. In particular, for SN 2002ap, $v_{\rm ej,b} \approx 2 \times 10^4$ km s^{-1}, which is lower than the velocity of the ejecta producing the radio emission, $v \approx 9 \times 10^4$ km s^{-1} (Berger et al. 2002b). Similarly, for SN 1998bw $v_{\rm ej,b}$ ranges from about 1.5×10^4 to 3.5×10^4 km s^{-1} (depending on which model is assumed, Table 8.2) while the radio emission was produced by ejecta expanding with $\Gamma\beta \approx 2$.

The ejecta velocity profile extends up to a cutoff determined by significant radiative losses when the shock front breaks out of the star. For a radiative stellar envelope this is $v_{\rm ej,max} \approx 11.5 \times 10^4 E_{K,51}^{0.58} M_{\rm ej,1}^{-0.42}$ (Matzner & McKee 1999), assuming a stellar radius of 1 R$_\odot$. For the SNe considered here we find cutoff velocities of $\Gamma\beta \sim 1 - 3$.

To determine whether there is sufficient energy in fast ejecta to account for the radio observations we calculate the energy above a velocity, V (Matzner & McKee 1999):

$$E(v > V) \approx \int_V^\infty \frac{1}{2} \rho_f v^2 4\pi v^2 t^3 dv \approx 7.2 \times 10^{44} E_{K,51}^{3.59} M_{\rm ej,1}^{-2.59} V_5^{-5.18} \, {\rm erg}, \quad (8.3)$$

where V_5 is the velocity in units of 10^5 km s^{-1}.

Unfortunately, as can be seen from Table 8.2, only four (including SN 1998bw) SNe have sufficient optical data which is necessary to estimate E_K and $M_{\rm ej}$. Of this limited sample, much of the radio data for SN 1994I remain unpublished. Thus we are left with SN 2002ap, SN 1983N, and SN 1998bw.

Using the parameters given in Table 8.2 for SN 2002ap, Berger et al. (2002b) find $E(v > 0.3c) \approx 3.8 \times 10^{48}$ erg. In contrast, from the radio observations we estimate 2×10^{46} erg. Thus, there is no need, nor indeed room, for mildly relativistic ejecta in this SN. We therefore disagree with the claims of high velocity jets carrying a large amount of energy, $\sim 0.1 - 1$ FOE, made by Kawabata et al. (2002) and Totani (2003). Furthermore, the large discrepancy between the amount of energy inferred from the hydrodynamic models and the radio observations suggests that either the optically-derived parameters are in error, Equation 8.3 has an incorrect pre-factor, or the radio estimate is incorrect. However, the radio estimate is relatively robust (eventually related to equipartition energy estimates). On the other hand, as with SN 1998bw (Höflich et al. 1999) the total kinetic energy may have been over-estimated, possibly as a result of neglecting a mild asymmetry.

For SN 1984L we do not have a direct estimate of the energy in the radio-emitting ejecta since the peak of the radio emission has been missed. However, based on the similarity to SN 1983N in the optically thin regime we estimate $L_p(t = 30\,{\rm d}, \nu_p = 5\,{\rm GHz}) \approx 1.4 \times 10^{27}$ erg s^{-1} Hz^{-1}. This translates to a peak flux of 3.2 mJy at the distance of SN 1984L ($d \approx 19$ Mpc). Using the equipartition analysis presented in §8.6.3 we estimate an energy of about 7×10^{46} erg, and an average expansion velocity of about $0.1c$. From Equation 8.3 we find $E(v > 0.1c) \approx 3 \times 10^{50}$ erg – similar to the conundrum discussed above for SN 2002ap.

For SN 1998bw, on the other hand, we find $E(v > c) \approx 2 \times 10^{45}$ erg using the parameters inferred by Höflich et al. (1999), or $E(v > c) \approx 3 \times 10^{48}$ erg using the parameters given by Iwamoto et al. (1998). In both cases, the energy available in fast ejecta is significantly lower than the energy inferred from the radio emission, $\sim 10^{50}$ erg.

To conclude, for SN 1984L and SN 2002ap a hydrodynamic explosion can supply the energy and velocity that are responsible for the observed radio emission. Most likely, the same is true for the non-detections. On the other hand, SN 1998bw is a clear exception, exhibiting a significant excess of energy in ejecta moving with $\Gamma\beta \approx 2$ compared to what is available from a hydrodynamic explosion.

SECTION 8.4

A Comparison to γ-Ray Burst Afterglows

In the previous section we investigated the radio properties of Type Ib/c SNe and found that in every respect SN 1998bw was unique. In this section we compare the Ib/c sample (including SN 1998bw)

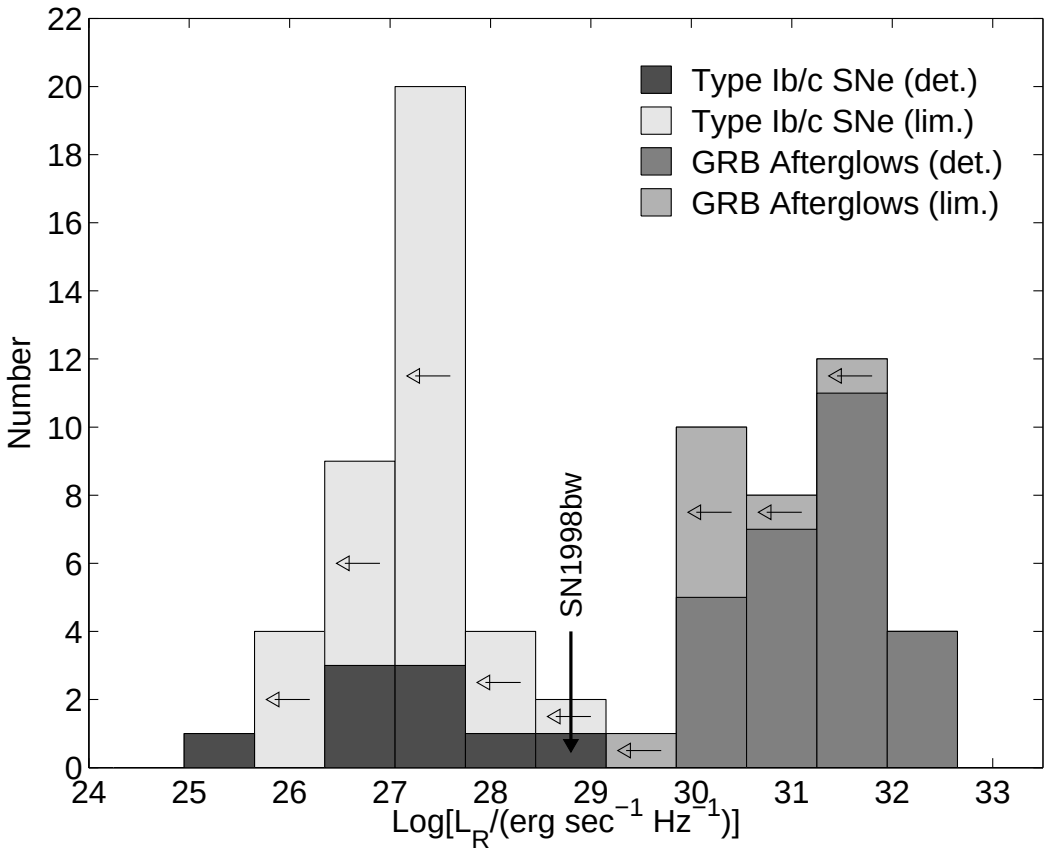

Figure 8.4: Histograms of the radio luminosity of Type Ib/c SNe from this survey and the literature, and GRB radio afterglows from the sample of Frail et al. (2003). Upper limits are plotted as 3σ, unless there is significant contamination from the host galaxy (see Table 8.1).

with the radio afterglows of GRBs. In Figure 8.2 we plot the radio light curves of GRB 970508 (Frail et al. 2000c), a typical cosmological burst, and the nearest event, GRB 030329 (Berger et al. 2003c), in addition to the SN light curves. As demonstrated by this figure and Figure 8.4, the radio light curves of GRB afterglows and SNe are dramatically different. Furthermore, SN 1998bw is unique in both samples: it is fainter than typical radio afterglows of GRBs but much brighter than Type Ib/c SNe.

Figures 8.2 and 8.4 have significant implications, namely, *none* of the Type Ib/c SNe presented here could have given rise to a typical γ-ray burst. It has been suggested that GRBs are distant Type Ib/c SNe but with their jets pointed at the observer, whereas such a bias is absent in the nearby Type Ib/c sample. However, most of our radio observations are obtained on a timescale of 10–100 days (see Figure 8.1). Scaling from the observed "jet" break times of a few days in GRB afterglows, off-axis collimated explosions become spherical on a timescale of $\sim 10 - 10^2$ days (Paczynski 2001; Granot & Loeb 2003) at which point the relative geometry between the observer and the explosion is not important. Thus, we find no evidence suggesting that all or even a reasonable majority of Type Ib/c SNe give rise to GRBs. We now quantify the difference between the Ib/c and GRB samples.

Our goal here is to determine the differential luminosity distribution, $n(L)$, which agrees with both detections and upper limits; here $n(L)$ is the number of events with luminosity between L and $L + dL$. It is important to include non-detections since they represent the majority of the SN data. Similarly, we include upper limits on the radio luminosity of GRB afterglows that have been localized in other wave-bands (i.e., optical and X-rays) and for which a redshift has been measured. Unfortunately, as many as half of the GRBs localized in the X-rays do not have a precise position, and hence a redshift. For these afterglows it is not possible to provide a limit on the radio luminosity. Still, with a typical

flux limit of about 0.3 mJy (5σ; Frail et al. 2003a), and assuming that these sources have a similar distribution of redshifts to the detected afterglows, we find typical luminosity limits of about 10^{31} erg s^{-1} Hz^{-1}, consistent with the peak of the distribution of detected afterglows. Therefore, unless these sources are biased to low redshift we do not expect a strong bias as a result of neglecting them.

The quality of fit for $n(L)$ is determined using the Likelihood function, $\mathcal{L} = \prod_{i=1}^{N} \mathcal{L}_i$, with (Reichart & Yost 2001):

$$\mathcal{L}_i = \begin{cases} \int_{-\infty}^{\infty} n(L)\mathcal{G}(L_i, \sigma_{Li})dL & L_i = detection \\ \int_{L_i}^{\infty} n(L)dL & L_i = limit, \end{cases} \tag{8.4}$$

where N is the total number of sources (SNe or afterglows), and $\mathcal{G}(L_i, \sigma_{Li})$ is a normalized Gaussian profile centered on the observed luminosity of a detected source and with a width equal to the 1σ rms uncertainty in the luminosity.

We consider four models for $n(L)$ based on the apparent distribution of the detections and upper limits: a Gaussian,

$$n(L) = \frac{1}{\sqrt{2\pi}\sigma_L} \exp\left[-\frac{1}{2}\left(\frac{L - L_0}{\sigma_L}\right)^2\right], \tag{8.5}$$

a decreasing power-law,

$$n(L) = \begin{cases} 0 & L < L_0 \\ (1 - \alpha_L)L^{\alpha_L}/(L_0^{\alpha_L+1}) & L \geq L_0, \end{cases} \tag{8.6}$$

an increasing power-law,

$$n(L) = \begin{cases} (1 + \alpha_L)L^{\alpha_L}/(L_0^{\alpha_L+1}) & 0 \leq L < L_0 \\ 0 & L \geq L_0, \end{cases} \tag{8.7}$$

and a flat distribution,

$$n(L) = \begin{cases} 0 & L < L_1 \\ 1/(L_2 - L_1) & L_1 \leq L \leq L_2 \\ 0 & L > L_2. \end{cases} \tag{8.8}$$

In each case we fit for the two free parameters (e.g., L_0 and σ_L in Equation 8.5). We do not use the increasing power law model for the individual distributions since the observations are clearly inconsistent with such a model. The resulting best-fit models are shown in Figure 8.5 and summarized in Table 8.3.

We find that the SN population is modeled equally well with the Gaussian, flat, or decreasing power law distributions, while the GRB afterglows can be fit with a Gaussian or flat distributions; a decreasing power law provides a much poorer fit. Regardless of the exact distribution the two populations require distinctly different parameters, with a minimal overlap at the tails of the distributions.

Fitting the combined SN and afterglow data with the models provided above (Figure 8.5 and Table 8.3) we find that even the best models (an increasing power-law or a flat distribution) provide a much poorer fit; the likelihood of the fits are $\ln(\mathcal{L}) \approx 104$ compared to the combined value of 61.3 for the separate Gaussian fits. Thus, the two populations cannot be accommodated with a simple single distribution. This points to a separate origin for the GRB and Type Ib/c SN populations. However, SN 1998bw can be accommodated in either population. It is equally plausible that it is a low luminosity GRB or the brightest Type Ib/c radio supernova known to date.

SECTION 8.5

Discussion and Conclusions

We presented VLA radio observations of 33 Type Ib/c SNe observed between late 1999 and the end of 2002. Four of these SNe have been detected, giving a detection rate of about 12% above a typical 3σ

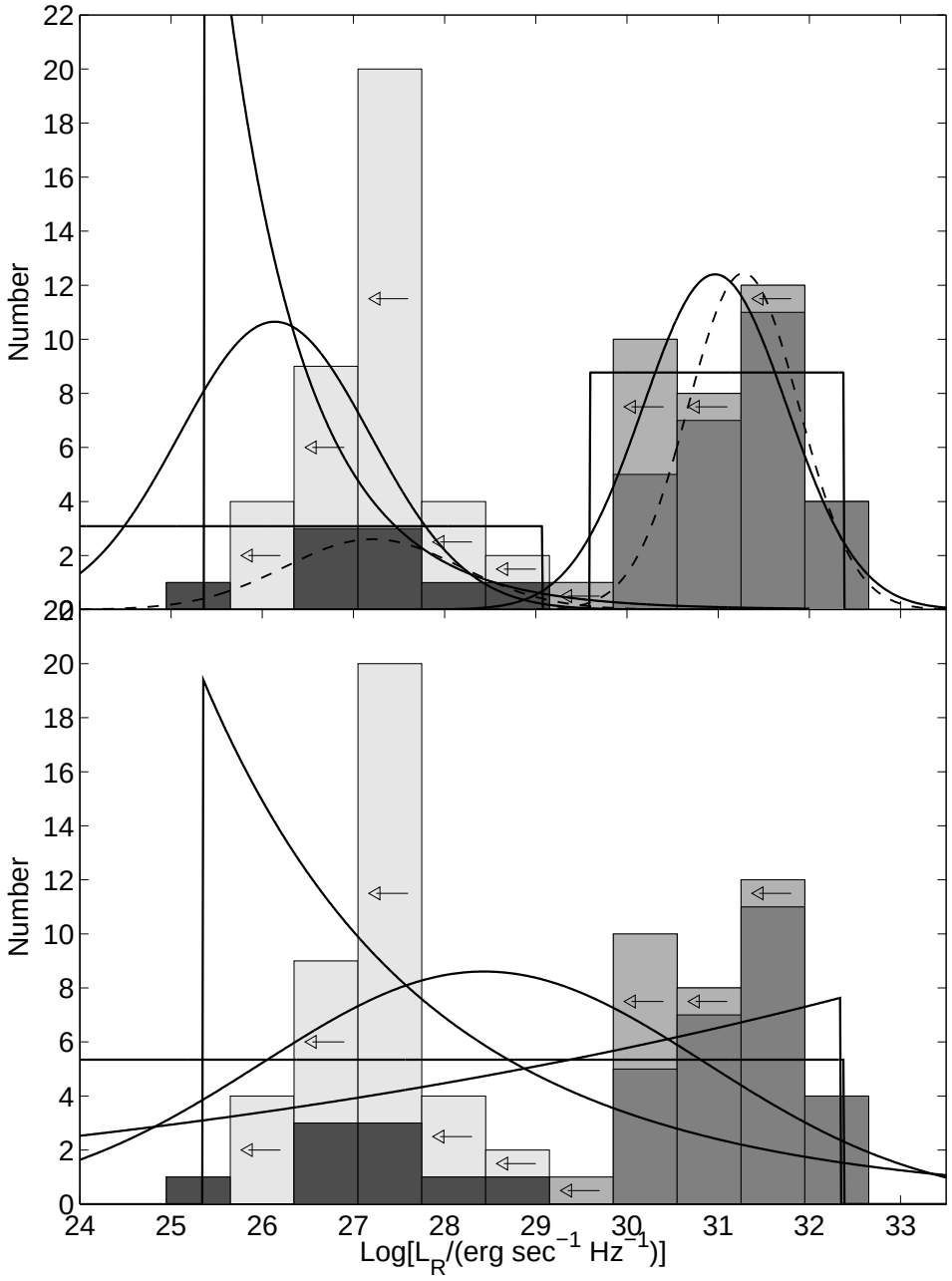

Figure 8.5: Same as Figure 8.4 but with models of the luminosity distribution (§8.4). The dashed lines are a Gaussian profile fit for the detections in each sample. The solid lines are a fit to the detections and upper limits using several models for the distribution function (§8.4). In the top panel we model each population separately, whereas the bottom panel shows models for the combined populations. No single distribution can fit both the local Type Ib/c SN population and the cosmological GRB population (Table 8.3).

flux limit of 0.15 mJy. At the same time, the combined detections and non-detections indicate that at most 3% of Type Ib/c SNe are as luminous as SN 1998bw, although the single source which may be brighter is only so because it is embedded in a radio bright host galaxy.

We infer typical velocities of the radio-emitting ejecta of about $10^4 - 10^5$ km s^{-1} for the detected SNe, and upper limits in the same range for the non-detections. We also find that a hydrodynamic explosion can supply the energy carried by the fastest ejecta. Finally, none of the detected SNe show

clear evidence for variable energy input (shells with different velocity or continued activity by the central engine); however, we note that our sampling is quite sparse.

The measurements (radio light curves) and inferences (energy in fast ejecta, energy addition) offer no compelling reason to conclude that any of our SNe have the special properties of SN 1998bw (§8.5.1).

Norris (2002) has proposed, based on the empirical lag-luminosity relation, that 25% of Type Ib/c SNe are similar to SN 1998bw. Clearly, this conclusion is not borne out by observations. This may indicate that the lag-luminosity relation does not apply to bursts with long lags (i.e., low luminosity) which comprise the local sample of Norris (2002)

We also compared the Type Ib/c sample with the sample of radio afterglow of GRBs. Empirically, these two populations appear to be quite disparate. This conclusion is reinforced by careful modeling of the luminosity distributions. Still, SN 1998bw may belong to either population.

8.5.1 What Is SN 1998bw?

Our four year survey of Type Ib/c SNe was first and foremost motivated by the peculiar object, SN 1998bw. This supernova showed three attributes unique to GRBs: relativistic ejecta, substantial reservoir of energy in such ejecta, and energy addition. A singular hydrodynamic explosion cannot account for these attributes. A natural explanation is that SN 1998bw, like GRBs, was driven by an engine powerful enough to significantly modify the explosion.

Our survey has demonstrated that SN 1998bw-like events are rare in the local sample. This begs the question: what is SN 1998bw?

Two popular scenarios have been suggested. The first – the "off-axis" scenario – holds that SN 1998bw is a typical GRB albeit nearby and with collimated ejecta pointed away from us (MacFadyen & Woosley 1999; Nakamura 1999; Granot et al. 2002). This hypothesis is attractive because of its simplicity. We know GRBs exist and most of them do not point towards us (Frail et al. 2001).

In the other scenario SN 1998bw is a new type of explosion (GRB supernovae, or gSN) with little energy in ultra-relativistic ejecta (Bloom et al. 1998b; Kulkarni et al. 1998; Höflich et al. 1999). Evidence in favor of this idea is best illustrated by Figure 8.6 where we find that GRB 980425 is consistently at the faint end of the GRB population.

Unfortunately, we are not able to decisively resolve this controversy. As demonstrated by Figure 8.4, one could argue that SN 1998bw is at the bright end of the radio luminosity function of Type Ib/c supernovae or at the faint end of GRB radio afterglow.

The expected rate of SN 1998bw-like events in the off-axis framework is about 0.5% of Type Ib/c events, given the average beaming factor of about 500 derived by Frail et al. (2001). Thus, it is not entirely improbable that one out of about 40 Type Ib/c SNe observed to date is an off-axis GRB. As an aside, we can use our 3% limit and compare the event rate of Type Ib/c SNe with the observed rate of GRBs (§8.1) to place a limit of $f_b \gtrsim 3 \times 10^{-4}$ on the beaming fraction. This corresponds to a limit of $\theta_j \gtrsim 1.4^\circ$ on the jet opening angles of GRBs; narrower jets are not likely. This result may also be interpreted as a limit on angular size of the highly relativistic core in models of variable energy and/or Lorentz factor across the surface of the jet (Rossi et al. 2002; Zhang & Mészáros 2002).

In the gSN framework, we now know that at most a few percent of Type Ib/c are possibly gSNe. At the same time, the recent GRB 030329 was accompanied by a SN similar to SN 1998bw (SN 2003dh; Stanek et al. 2003; Hjorth et al. 2003). Thus, an investigation of the number and properties of gSNe requires observations of both local Type Ib/c SNe and GRBs.

While we cannot determine the exact origin of SN 1998bw based on the statistics of our survey, the ultimate detection of similar events at the level of about 1% may in fact allow us to distinguish between the off-axis and gSN scenarios.

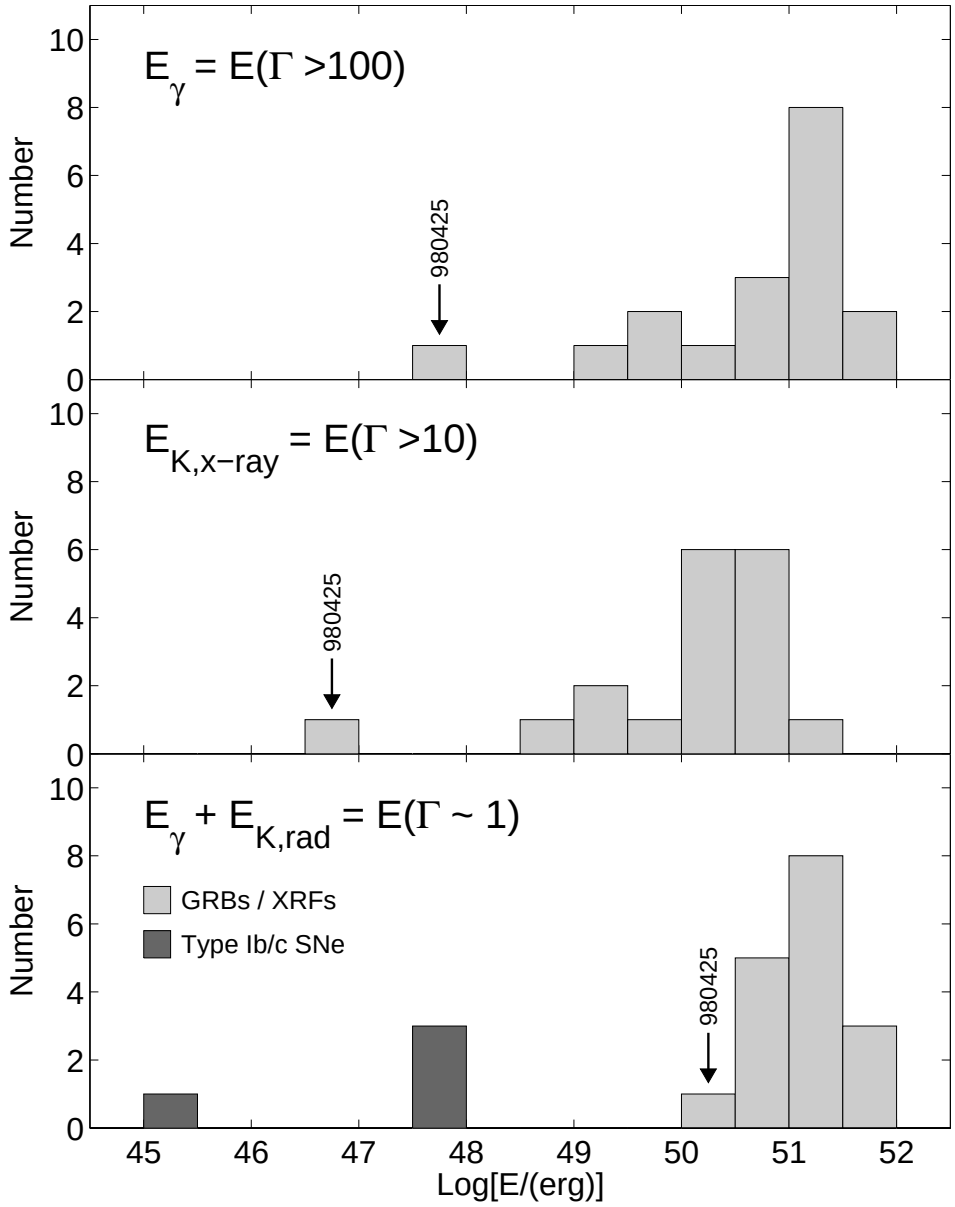

Figure 8.6: Histograms of the beaming-corrected γ-ray energy (Bloom et al. 2003b), E_γ, the kinetic energy inferred from X-rays at $t = 10$ hr (Berger et al. 2003a), $E_{K,X}$, and total relativistic energy, $E_\gamma + E_K$, where E_K is the beaming-corrected kinetic energy inferred from the broad-band afterglows of GRBs (Li & Chevalier 1999; Panaitescu & Kumar 2002) and radio observations of SNe. The wider dispersion in E_γ and $E_{K,X}$ compared to the total energy indicates that engines in cosmic explosions produce approximately the same quantity of energy, thus pointing to a common origin, but the ultra-relativistic output of these engines varies widely. In Type Ib/c SNe, on the other hand, the total explosive yield in fast ejecta (typically $\sim 0.3c$) is significantly lower. This points to a separate origin for these two explosive phenomena.

8.5.2 Hypernovae

The discovery of broad optical lines in SN 1998bw and large explosive energy release, $\gtrsim$ few FOE, prompted some astronomers to use the designation "hypernovae" for SN 1998bw-like SNe. Unfortunately, this designation is not well defined. To begin with, the term hypernova was first used by Paczynski (1998) to describe the GRB/afterglow phenomenon; thus, this term implies a connection to

GRBs. The prevalent view now is that hypernovae are characterized by broad optical absorption lines and larger than normal energy release. However, neither of these criteria has been defined quantitatively by their proponents.

Ignoring this important issue, the following have been suggested to be hypernovae: the Type Ib/c SNe 1992ar (Clocchiatti et al. 2000), 1997dq (Matheson et al. 2001a), 1997ef (Iwamoto et al. 2000; Mazzali et al. 2000), 1998ey (Garnavich et al. 1998), and 2002ap (Mazzali et al. 2002), and the Type II SNe 1992am (Hamuy 2003), 1997cy (e.g., Germany et al. 2000), and 1999E (Rigon et al. 2003). Some have also been claimed to be associated with GRBs detected by BATSE, but at a low significance.

Our view is that the critical distinction between an ordinary supernova and a GRB explosion are relativistic ejecta carrying a considerable amount of energy. Such ejecta are simply not traced by optical spectroscopy. This reasoning is best supported by the fact that the energy carried by the fast ejecta in SN 1998bw and SN 2002ap (Berger et al. 2002b) differ by four orders of magnitude even though both exhibit broad spectral features at early times (see also Wang et al. 2003). Thus, broad lines do not appear to be a good surrogate for SN 1998bw-like objects.

In addition, in two cases, SNe 2002ap and 1984L, the energy inferred from the radio observations indicates that the total kinetic energy as inferred by optical spectroscopy and light curves may have been over-estimated by an order of magnitude (§8.3.3). It is possible that "hypernovae" are in fact only slightly more energetic than typical Type Ib/c SNe, but exhibit a mild degree of asymmetry, leading to excessively high estimates of the total energy when a spherical explosion is assumed.

We suggest that the term hypernova be reserved for those SNe, like SN 1998bw, which show direct evidence for an engine through the presence of relativistic ejecta. As illustrated by SN 1998bw, the relativistic ejecta are reliably traced by radio observations.

We end with the following conclusions. First, radio observations provide a robust way of measuring the quantity of energy associated with high velocity ejecta. This allows us to clearly discriminate between engine-driven SNe such as SN 1998bw and ordinary SNe, powered by a hydrodynamic explosion, such as SN 2002ap (Berger et al. 2002b) and SNe 2001B, 2001ci, and 2002cj presented here. Second, since at least 97% of local Type Ib/c SNe are not powered by inner engines and furthermore have a total explosive yield of only 10^{48} erg in fast ejecta (where fast means $v \sim 0.3c$ compared to $\Gamma \sim few$ in GRBs), there is a clear dichotomy between Type Ib/c SNe and cosmic, engine-driven explosions (Figure 8.6). The existence of intermediate classes of explosions and the nature of SN 1998bw may be ascertained with continued monitoring of several hundred Type Ib/c SNe and cosmological explosions. Fortunately, such samples will likely become available over the next few years.

SECTION 8.6

Results for Individual Supernovae

8.6.1 SN 2001B

SN 2001B was discovered in images taken on 2001, Jan 3.61 and 4.57 UT, approximately 5.6 arcsec west and 8.9 arcsec south of the nucleus of IC 391 (Xu & Qiu 2001). The SN explosion occurred between 2000, Dec 24.54 UT and the epoch of discovery. Based on an initial spectrum, taken on 2001, Jan 14.18 UT Matheson et al. (2001b) concluded that the SN was of Type Ia approximately 9 days past maximum brightness, showing well defined Si II and Ca II features, with a Si II expansion velocity of about 7400 km sec^{-1}. A subsequent spectrum taken on 2001, Jan 23 indicated that the SN was in fact of Type Ib based on clear He I absorption lines (Chornock & Filippenko 2001).

We observed SN 2001B on 2001, Feb 4.49 UT at 8.46 GHz. An initial analysis revealed a source which was interpreted as the host galaxy of the SN, with a flux of 3.5 mJy. A second epoch obtained on 2002, Oct 28.45 UT revealed that the source had faded below 0.12 mJy, establishing it as the radio counterpart of SN 2001B. (Figure 8.1).

8.6.2 SN 2001ci

SN 2001ci was initially detected in images taken with the Katzman Automatic Imaging Telescope on 2001 Apr 25.2 UT, 6.3 arcsec west and 25.4 arcsec north of NGC 3079 (Swift et al. 2001). These observations did not provide conclusive evidence that the source was in fact a SN. A spectrum obtained by Filippenko & Chornock (2001) on 2001, May 30 UT revealed that the source was in fact a Type Ic SN about $2-3$ weeks past maximum brightness (Matheson et al. 2001a).

We observed the SN on 2001, Jun 6.35 UT at 8.46 GHz, but did not detect the source since it appeared to be part of the host galaxy extended structure. A second epoch taken on 2002, Jun 10.9 UT revealed a clear fading at the optical position of the SN with a flux of 1.45 ± 0.25 mJy in the first epoch, and a 2σ limit of 0.3 mJy in the second epoch.

8.6.3 SN 2002cj

SN 2002cj was discovered on 2002, Apr 21.5 UT, 1.4 arcsec west and 3.9 arcsec south of the nucleus of ESO 582-G5, at a distance of 106 Mpc (Ganeshalingam & Li 2002). The SN explosion occurred between Apr 9.5 UT and the epoch of discovery. Spectra of the SN obtained on 2002, May 2.43 and May 7 UT revealed that SN 2002cj is of Type Ic (Matheson et al. 2002; Chornock 2002).

We initially observed the SN on 2002, Jun 3.19 UT at 1.43, 4.86, and 8.46 GHz and detected a faint source at all three frequencies. The SN spectrum is given by $F_\nu \propto \nu^{-0.1\pm0.3}$ between 1.43 and 4.86 GHz, and $F_\nu \propto \nu^{-1.2\pm0.8}$ between 4.86 and 8.46 GHz, indicating that the spectral peak was most likely located between 1.43 and 4.86 GHz during the first epoch ($\Delta t \approx 43-55$ days). In subsequent observations at 1.43 GHz the SN brightened and then faded, as expected if the peak was in fact above 1.43 GHz initially, and shifted through the band at later epochs. Using the expected shape of the spectrum, $F_\nu \propto \nu^{5/2}$ for $\nu < \nu_p$ and $F_\nu \propto \nu^{-(p-1)/2}$ for $\nu > \nu_p$ (with $p \sim 3$), we find $F_{\nu,p} \sim 0.5$ mJy at $\nu_p \sim 2$ GHz and $\Delta t = 43-55$ days.

We use these values along with the well-established equipartition analysis (Readhead 1994) to derive some general constraints on the properties of the emitting material. In particular, the energy of a synchrotron source with flux density, $F_p(\nu_p, t_p)$, can be expressed in terms of the equipartition energy density,

$$\frac{U}{U_{\rm eq}} = \frac{1}{2}\epsilon_B \eta^{11}(1 + \frac{\epsilon_e}{\epsilon_B}\eta^{-17}), \tag{8.9}$$

where $\eta = \theta_s/\theta_{\rm eq}$, the equipartition size is $\theta_{\rm eq} \approx 120 d_{\rm Mpc}^{-1/17} F_{p,{\rm mJy}}^{8/17} \nu_{p,{\rm GHz}}^{(-2\beta-35)/34}$ μas, $U_{eq} = 1.1 \times 10^{56} d_{\rm Mpc}^2 F_{p,{\rm mJy}}^4 \nu_{p,{\rm GHz}}^{-7} \theta_{{\rm eq},\mu{\rm as}}^{-6}$ erg, and ϵ_e and ϵ_B are the fractions of energy in the electrons and magnetic fields, respectively. In equipartition $\epsilon_e = \epsilon_B = 1$ and the energy is minimized; a deviation from equipartition will increase the energy significantly.

For SN 2002cj we find $\theta_{\rm eq}(t = 43-55\,{\rm d}) \approx 30$ μas (i.e., $R_{\rm eq} \approx 5 \times 10^{16}$ cm), which indicates an average expansion velocity, $v_{\rm eq} \approx (0.35-0.45)c$. The equipartition energy is $U_{\rm eq} \approx 8 \times 10^{47}$ erg, indicating a magnetic field strength of $B_{\rm eq} \approx 0.2$ G.

We thank B. Paczynski, B. Schmidt, C. Wheeler and the referee for helpful comments. GRB and SN research at Caltech is supported in part by funds from NSF and NASA.

Table 8.1. Radio Observations of Type Ib/c Supernovae in the Period 1999-2002

SN	IAUC	t_0 (UT)	$t_{\rm obs}$ (UT)	Δt (days)	Dist. (Mpc)	Detected?	$F_{8.46}$ (μJy)	$F_{4.86}$ (μJy)	$F_{1.43}$ (μJy)
1999ex	7310	Oct 25.6–Nov 9.5	Nov 18.02	8.5–23.4	54	No	$\pm 53^a$	± 71	—
2000C	7348	1999 Dec 30–2000 Jan 8.3	Feb 4.04	26.7–36.0	59	Hint	—	187 ± 84	—
2000F	7353	1999 Dec 30.3–Jan 10.2	—	—	92	—			
2000S	7384	<Feb 28^b	—	—	94	—			
2000cr	7443	Jun 21.2–25.9	Jul 3.04	7.1–11.8	54	No	$\pm 42^c$	—	—
2000de	7478	Jun 6–Aug 10.9	—	—	39	—			
2000ds	7507	May 28–Oct 10.4	—	—	21	—			
2000dt	7508	Sep 21–Oct 13.1	—	—	107	—			
2000dv	7510	<Oct 17.1	—	—	63	—			
2000ew	7530	May 8–Nov 28.5	2002 Jun 26	575–780	15	No	—	—	± 67
2000fn	7546	Nov 1–19	Dec 29.22	40.2–58.2	72	No	± 45	—	—
2001B	7555	2000 Dec 24.5–Jan 3.6	Feb 4.49	31.9–42.0	24	Yes	3500 ± 29	—	—
			2002 Oct 28.45	672.9–683		No	± 40	—	—
2001M	7568	Jan 3.4–21.4	Feb 4.45	14.1–32.1	56	No	± 28	—	—
2001ai	7605	Mar 19.4–28.4	Mar 31.36	3–12	118	No	$\pm 43^f$	$\pm 49^f$	$\pm 49^f$
2001bb	7614	Apr 15.3–29.3	May 5.26	6–20	72	No	± 50	± 60	± 120
2001ch	7637	2000 Nov 28.3–May 28.5	—	—	46	—			
2001ci	7618	Apr 17.2–25.2	Jun 6.35	42.2–50.2	17	Yes	1450 ± 250	—	—
			2002 Jun 10.90	411.7–419.7		No	± 150	—	—
2001ef	7710	Aug 29–Sep 9.1	Sep 14.3	5.2–16.3	38	No	$\pm 115^g$	—	—
			2002 Jun 18.0	281.9–293		No	—	—	± 88
2001ej	7719	Sep 1–17.1	Sep 27.25	10.6–26.7	63	No	$\pm 44^h$	—	—
			2002 Jun 14.0+18.0	269.9–469		No	—	—	± 85
2001em	7722	Sep 10.3–15.3	—	—	91	—			
2001eq(?)	7728	Aug 31.3–Sep 12.3	—	—	118	—			
2001fw	7751	Oct 26–Nov 11.2	—	—	139	—			
2001fx	7751	Oct 14.2–Nov 8.2	—	—	126	—			
2001is	7782	Dec 14–23	2002 Jun 14.0+18.0	175–184	60	No	—	—	$\pm 70^i$
2002J	7800	Jan 9.4–21.4	Jun 18.0	147.6–159.6	58	No	—	—	± 85
2002ap^j	7810	Jan 28.5	Feb 1.03	3.5	7	Yes	374 ± 29	—	—
2002bl	7845	Feb 14–Mar 2.9	Mar 8.26	6–22	74	No	± 50	± 45	—
2002bm	7845	Jan 16–Mar 6.2	Jun 26.0	111.8–161	85	No	—	—	± 66
2002cg	7877	Mar 28.5–Apr 13.5	Jun 26.0	73.5–89.5	150	No	—	—	$\pm 74^k$

Table 8.1

SN	IAUC	t_0 (UT)	$t_{\rm obs}$ (UT)	Δt (days)	Dist. (Mpc)	Detected?	$F_{8.46}$ (μJy)	$F_{4.86}$ (μJy)	$F_{1.43}$ (μJy)
2002cj	7882	Apr 9.5–21.5	Jun 3.19	42.7–54.7	106	Yes	112 ± 33	220 ± 37	240 ± 48
			Jun 18.0	57.5–69.5		Yes	—	—	408 ± 81
			Jun 26.0	65.5–77.5		Yes	—	—	300 ± 68
2002cp	7887	Apr 11.2–28.2	Jun 1.96	34.8–51.8	80	No	± 31	± 35	± 36
2002cw	7902	2001 Oct 1.2–May 16.5	—	—	71	—			
2002dg	7915	2002 May 5–May 31.3	Jul 9.95	39.7–66	215[l]	Hint	± 33	92 ± 37	± 46
2002dn(?)	7922	May 31.5–Jun 15.5	Jul 4.4	18.9–33.9	115	No	± 39	± 43	± 72
2002dz	7935	2001 Nov 10.2–Jul 16.5	—	—	84	—			
2002ex	7964	Aug 19.3	—	—	180	—			
2002fh(?)	7971	Apr 9–May 9.3	—	—	1870	—			
2002ge(?)[m]	7987	2000 Oct 1.8–2002 Oct 7.9	Oct 12.0	~ 13	47	No	± 160[n]	± 130[o]	—
2002gy	7996	Oct 9.4–16.4	Oct 28.45	19.1–26.1	114	No	± 36	± 39	—
2002hf	8004	Oct 22.3–29.3	Nov 7.17	8.9–16.9	88	No	± 40	—	—
2002hn	8009	Oct 21.5–30.5	Nov 7.42	7.9–16.9	82	No	± 44	—	—
2002ho	8011	May 27–Nov 5.1	Nov 15.33	~ 56[p]	42	No	± 47	± 54	—
2002hy	8016	Oct 13.1–Nov 12.1	Nov 21.71	9.6–39.6	58	No	± 74	—	—
2002hz	8017	Nov 2.2–12.2	2003 Jan 21.09	69.9–70.9	85	No	± 29	—	—
2002ji	8025	Apr 10–Nov 30.8	Dec 5.67	38.4–59.4[q]	23	No	± 43	—	—
2002jj	8026	Oct 1.4–24.4	Dec 15.28	51.9–74.9	66	No	± 33	—	—
2002jp	8031	May 14.2–Nov 23.5	Dec 14.55	~ 33[r]	58	No	± 38	—	—
2002jz	8037	2001 Dec 5–2002 Dec 23.3	2003 Jan 3.28	~ 32[s]	24	No	± 25[t]	—	—

Note. — The columns are (left to right): (1) SN name, (2) IAU Circular number for the initial detection, (3) time of the SN explosion, with the range given between the most recent observation of the galaxy which did not show the SN and the epoch at which the SN was detected, (4) epoch of our VLA observations, (5) time delay between the SN explosion and the epoch of our observations, (6) distance to the galaxy (assuming $H_0 = 65$ km s^{-1} Mpc^{-1}), (7) indicates whether radio emission was detected, (8) flux density at 8.46 GHz, (9) flux density at 4.86 GHz, and (10) flux density at 1.43 GHz.

[a] uncertainties are quoted as 1σ rms; [b] nebular phase; [c] falls on top of galaxy substructure, $< 10\sigma$; [d] Ia or Ic (IAUC 7574); [e] before maximum (IAUC 7574); [f] falls on top of galaxy with complex substructure, $< 4\sigma$; [g] falls on top of galaxy, $< 5\sigma$; [h] falls on top of galaxy, $< 35\sigma$; [i] on top of galaxy substructure, $< 3\sigma$; [j] See Berger et al. (2002b); [k] on top of galaxy, $< 10\sigma$; [l] IAUC 7922; [m] Type Ic similar to SN 1994I a few days before maximum, or a sub-luminous Type Ia (IAUC 7990); [n] on top of galaxy, $< 10\sigma$; [o] on top of galaxy, $< 3\sigma$; [p] within a few weeks past maximum brightness (IAUC 8014); [q] $3 - 6$ weeks past maximum light (IAUC 8026); [r] two weeks past maximum light (IAUC 8031); [s] ten days past maximum (IAUC 8037); [t] on top of galaxy substructure, $< 3\sigma$.

Table 8.2. Ejecta and Progenitor Properties of Type Ib/c Supernovae Detected in the Radio

SN	E_K (10^{51} erg)	$M_{\rm ej}$ ($M_\odot$)	$M_{^{56}\rm Ni}$ ($M_\odot$)	$M_{\rm CO}$ ($M_\odot$)	$M_{\rm prog}$ ($M_\odot$)	Ref.
1984L	20	50	0.2	—	—	1
	—	10	—	—	—	2
	—	—	0.1	—	$20-30$	3
1994I	$1-1.4$	$0.9-1.3$	0.07	<1.5	<15	4
	—	0.9	0.07	1.35	—	5
	1	—	—	—	—	6
1998bw	30	—	0.7	13.8	40	7
	50	10	0.4	13.8	40	8
	22	—	0.5	6.5	—	9
	2	2	0.2	—	—	10
	—	—	$0.5-0.9^a$	—	—	11
2002ap	$4-10$	$2.5-5$	0.07	5	$20-25$	12

Note. — The columns are (left to right): (1) Ejecta kinetic energy, (2) ejecta mass, (3) ^{56}Ni mass, (4) estimated mass of the CO core, (5) estimated mass of the progenitor, and (6) references. Data are not available for the SNe detected in this survey. ^{a} These authors use the models of Iwamoto et al. (1998) and Woosley et al. (1999) as input; they assert that observations in the nebular phase exclude the low ^{56}Ni mass inferred by Höflich et al. (1999).

References. — (1) Baron et al. (1993); (2) Swartz & Wheeler (1991); (3) Schlegel & Kirshner (1989); (4) Young et al. (1995); (5) Iwamoto et al. (1994); (6) Millard et al. (1999); (7) Iwamoto et al. (1998); (8) Nakamura et al. (2001); (9) Woosley et al. (1999); (10) Höflich et al. (1999); (11) Sollerman et al. (2000); (12) Mazzali et al. (2002)

Table 8.3. Best-Fit Models for the Supernova and γ-Ray Burst Luminosity Distributions

Population	Model	Parameters	$\log(\mathcal{L})$/dof
SN	Gaussian	(26.1, 1.0)	22.5/36
SN	D. Powerlaw	(−29.0, 25.4)	22.4/36
SN	Flat	(20.0, 29.1)	22.3/36
GRB	Gaussian	(31.0, 0.8)	38.8/33
GRB	D. Powerlaw	(−22.5, 29.6)	48.9/33
GRB	Flat	(29.6, 32.4)	37.7/33
SN+GRB	Gaussian	(28.4, 2.4)	130.3/71
SN+GRB	D. Powerlaw	(−10.4, 25.3)	123.8/71
SN+GRB	I. Powerlaw	(3.7, 32.3)	103.7/71
SN+GRB	Flat	(22.6, 32.4)	104.9/71

Note. — The columns are (left to right): (1) Data set, (2) population distribution function, (3) best-fit parameters, and (4) log likelihood. A detailed explanation of the models and the fitting procedure is provided in §8.4.